Accepted Manuscript

<AT>Kinetics and reactive stripping modelling of hydrogen isotopic exchange of deuterated waters

<AU>Mohammed Aldehani[1], Faris Alzahrani[1], Meabh Nic An tSaoir[2], Daniel Luis Abreu Fernandes[3], Suttichai Assabumrungrat[4], Farid Aiouache[1*]
##Email##f.aiouache@lancaster.ac.uk##/Email##
<AU>
<AFF>Department of Engineering, Lancaster University, UK
<AFF>School of Chemistry and Chemical Engineering, Queen University Belfast, UK
<AFF>Department of Chemistry - Ångström Laboratory, Uppsala University, Sweden
<AFF>Centre of Excellence in Catalysis and Catalytic Reaction Engineering, Department of Chemical Engineering, Faculty of Engineering, Chulalongkorn University, Thailand

<PA>Tel.: +44 1524593526.

<ABS-HEAD>ABSTRACT
<ABS-P>This work presents results of experimental kinetics and modelling of the isotopic exchange between hydrogen and water in a reactive stripping column for water dedeuteriation. The missing physical properties of deuterium and tritium isotopologues in hydrogen gas and water forms were predicted and validated using existing literature data. The kinetic model relevant to a styrene-divinyl-benzene co-polymer–supported platinum catalyst was used for modelling, by Aspen plus modular package, impact of design parameters including temperature, total pressure, gas to liquid flowrate ratio, pressure drop and flow mixing, on the separation of deuterium and further the separation of tritium. The modelling by the rate-based non-equilibrium, including design correlations of model of mass and heat transfers, chemical kinetic constants, mass transfer coefficients and overall exchange rate constants, allowed access to separation trends in a good agreement with published data. The synergy between the rates of chemical isotopic exchange and gas/liquid mass transfer, and by inference the performance of reactive stripping, was particularly sensitive to high temperatures, low hydrogen flow rates, pressure drops and internals properties. Extension to tritium confirmed a slightly slower mass transport compared with deuterium leading to potentially under-estimated design features for detritiation processing when deuterium is used instead.
<KWD>Abbreviations: CECE Combined electrolysis and catalytic exchange, CEPE Chemical equilibrium - bulk gas/liquid physical equilibrium, CKEP Chemical kinetics - bulk gas/liquid physical equilibrium, CKRN-E Chemical kinetics - rate-based gas/liquid non-equilibrium, *DIPPR* Design Institute for Physical Properties Research, HETP *Height equivalent to theoretical plate [m],* I.D. Internal diameter [m], LPCE Liquid phase catalytic exchange, MESH Material balance, vapour–liquid equilibrium equations, mole fraction summations and heat balance, NSD Normalized standard deviation (%), PTFE Polytetrafluoroethylene, RadFrac Rate-based equilibrium separation process model, RateFrac Rate-based non-equilibrium separation process model, SDBC Styrene-divinylbenzene copolymer, SRK Soave-Redlich-Kwong equation-of-state

<KWD>Keywords: isotopic exchange; reactive stripping; detritiation; dedeuteriation; rate-based modelling; reactive separation

<td:DefL>Nomenclature
<xps:span class=deft>A Cross</xps:span> <xps:span class=defd>sectional area of the column [m^2]</xps:span>
<xps:span class=deft>a Interfacial area per unit bubbling area for trays [</xps:span> <xps:span class=defd>]</xps:span>
a_I Total interfacial area per unit volume of liquid, vapor [m^2/m^3]
a_F Specific area of the packing [m^2/m^3]
a_w Wetted surface area per unit volume of the column [m^2/m^3]

C_p Specific molar heat capacity [J/kmol K]

D Diffusivity [m²/s]

d_F Nominal packing size [m]

d_p Bed particle diameter [m]

d_s Sphere diameter [-]

Fr Froude number [-]

g Acceleration due to gravity [m.s⁻²]

G' Gas flow rate [mol/s]

G'/L' Gas to liquid flowrate ratio [-]

G Matrix of thermodynamic factors [-]

H Liquid enthalpy [J/mol]

h Vapour enthalpy [J/mol]

h' Heat transfer coefficient [W/m.K]

h_F Height of a packed section [m]

K Equilibrium constant between phases [-]

$k_{r,i}$ Kinetic rate constant of reaction i [mol/kg.s]

k_i Film mass transfer coefficient of species i [mol/m³.s]

K_{eq} Equilibrium constant for isotope exchange [-]

$K_{g,overall}$ Gas/liquid rate constant

L' Liquid flow rate [mol/s]

m_c Mass of catalyst [kg]

N Number of stages in the LPCE column [-]

n Number of data points in the normalized standard deviation equation [-]

n_c Number of components [-]

NM Rate of mass transfer between phases [mol/s]

P Total pressure [Pa]

P_c Critical pressure [kPa]

q Heat transfer rate between phases [J/s]

r_i Rate of the isotopic exchange (mole/kg.s)

Re Reynolds number [-]

$Sep_{D,e}$ Separation factor [-]

Sc Schmidt number

T Temperature [K]

T_B Boiling point temperature [K]

T_c Critical temperature [K]

V_c Critical molar volume [cm³/mol]

V_b Molar volume at the boiling point (cm³/mol)

We Weber number [-]

x Mole fraction in the liquid phase [-]

x'_D Atom fraction of deuterium in the liquid water

y Mole fraction in the gaseous phase

y_{eq} Equilibrium composition of deuterium in hydrogen phase

y_D' Atom fraction of deuterium in hydrogen phase

Z_c Critical compressibility factor [-]

<td:DefL>Greek symbols

λ Thermal conductivity [W/m.K]

φ Fugacity coefficient [-]

ϕ Fractional hole area per unit bubbling area [-]

μ Dynamic viscosity [Pa.s]

ν Kinematic viscosity [cP]

ρ Density [kg. m^{-3}]

σ Liquid surface tension [N/m]

σ_c Critical surface tension of packing [N/m]

δ Kronecker delta: 1 if i=k, 0 otherwise

ε Bed voidage [-]

<td:DefL>Subscripts

D_2 Deuterium gas

D_2O Heavy water or (deuterium oxide)

DT Deuterated tritium gas

DTO Tritiated heavy water

eq Equilibrium state

G Gas

HD Deuterated hydrogen

HDO Deuterated water

HT Tritiated hydrogen gas

I Interphase boundary between the gas and liquid HTO Tritiated water

L Liquid

T_2O Tritium oxide or (super-heavy water)

T_2 Tritium gas

V Vapour

1. Introduction

With energy demand growing at an alarming rate, nuclear energy has the potential to provide a long-term environmentally responsible solution for base-load electricity production. Next nuclear implementation strategy is envisioned as consisting of fusion power plants which include high temperature heat transfer loops for energy delivery [1]. These reactors contain passive safety features and are capable of withstanding postulated long-term, depressurized and loss–of–forced–convection accidents without damaging the fuel. However, radioactive effluents will be generated, mainly in the form of mixtures of tritiated and deuterated waters (i.e. HDO_L, HTO_L, DTO_L, T_2O_L and D_2O_L) and gases (i.e. DT, HT, HD, D_2 and T_2), at levels over ten thousand times higher than those produced by existing light water reactors [2]. There is evidence of adverse health effects on populations living near tritium facilities, owing to facile wall permeation by tritium even in low levels under the operated temperatures [1]. The simplest solution to preventing tritium contamination of downstream facilities is to deploy detritiation systems on the heat transfer fluid loops between the facilities and the utility systems but the management of these detritiation systems remains one of the main technological challenges for future industrial development [3].

The recovery of tritium in the forms of DTO_L, HTO_L or T_2O_L is an important process, not only because it allows for the reduction of concentration of the radiation hazard of intermediate level wastes, but also because tritium is a precious element for fusion reactions, and tritium recovery can help offset the high costs of disposal and storage [4]. Various technologies have been developed for water detritiation, including combined electrolysis and chemical exchange (CECE), liquid hydrogen distillation, cryogenic adsorption, palladium membrane diffusion, thermal diffusion, laser separation and electrochemical isotope separation [5-7]. The CECE process combines a water electrolysis unit and a liquid phase exchange (LPCE) column in which the catalytic hydrogen exchange reaction and the vapour/liquid scrubbing process occur. In the CECE, the contaminated water is first fed into an electrolyser where it is split into gaseous oxygen and hydrogen gases (H_2,

HD, T_2, D_2, HT and DT). The stream of hydrogen mixture is then directed up the LPCE column where it counter–currently interacts with water that is flowing down the catalytic packing column. As the liquid water trickles down the column, it becomes enriched in tritium while hydrogen gas becomes depleted, which causes an exchange of the HT/HD/T_2/D_2/DT gas with the scrubbing water to produce concentrated tritiated and deuterated waters (i.e. HDO_L, HTO_L, DTO_L, T_2O_L or D_2O_L) while H_2 is vented to the atmosphere. This catalytic exchange process is driven by two sets of isotopic exchange reactions: (1) a gaseous catalytic exchange between the hydrogen mixture and the stripped off water vapour (H_2O_V; reaction 1) and (2) the vapour–liquid concentration of the heavy water vapour isotopologues mixture HDO_V/HTO_V/DTO_V in liquid water (H_2O_L; reaction 2).

$$HD/HT/DT + H_2O_V \Leftrightarrow HTO_V/HDO_V/DTO_V + H_2 \qquad (1)$$
$$HTO_V/HDO_V/DTO_V + H_2O_L \Leftrightarrow HTO_L/HDO_L/DTO_L + H_2O_V \qquad (2)$$
This leads to the overall reaction:
$$HT/HD/DT + H_2O_L \Leftrightarrow HTO_L/HDO_L/DTO_L + H_2 \qquad (3)$$

The combined process, therefore, takes advantage of the wet scrubbing of HTO_V/HDO_V/DTO_V (produced by reaction 1)) by H_2O_L (as shown in reaction 2) and the reactive stripping of H_2O_V (produced by reaction 2) by hydrogen (as shown by reaction 1) to promote the rates and the equilibrium boundaries of both reactions. The catalytic reaction (1) is known to be weakly exothermic (-15.9 J/mol) and preferentially operates at mild temperatures [6]. It is also facilitated by hydrophobic or water-proof catalysts such as platinum, supported on carbons, polytetrafluoroethylene (PTFE) or resins (styrene-divinyl-benzene co-polymer (SDBC)) [8-13]. Reaction (2) expresses the liquid/vapour distillation exchange of mixture including water and heavy water isotopologues. This reaction is also known to be promoted at mild temperatures, since the associated enthalpy of evaporation of heavy water is higher than that of water, and is known to be kinetically accelerated by packing structures of a hydrophilic nature [4, 14, 15].

The hazards associated with handling tritium have promoted the development of extensive works aimed at modelling the overall process of the isotopic exchange for tritium detritiation. Most of the studies used assumptions based on average physical and transport properties while neglecting the thermal properties of isotopologues such as (heat of vaporization, enthalpy, heat capacity and conductivity) and the underlying heat transfer phenomena. The liquid stream in the LPCE column is typically operated under a trickle flow and a partial wetting of the packing, causing both mass and heat dispersions and a boundary resistance to mass transfer between liquid water and gaseous hydrogen. The methods for solving the multi-component reactive stripping/scrubbing system were mainly taken from the binary component approaches which are more or less straightforward extensions of methods that have been developed for solving conventional scrubbing/stripping column problems. Until recently, the trends of mass transfer rates of reaction 3 –, which lumps both the gaseous phase of reaction 1 and gas/liquid mass evaporation/condensation (reaction 2) – in a wet scrubbing/stripping column, have been the general objectives of most modelling studies. In studies on packed columns, the effects of the flow dynamics, counter–current stream ratios, temperature, pressure and type of packing internal have been recurrently cited [16].

In addition, the presence of chemical reactions in multicomponent separation systems influenced the component mass transfer with variations in each component in a complex and unpredictable way[22]. In reality, equilibrium was rarely attained and both stripping and scrubbing of tritium and deuterium deviated towards rate controlled phenomena, leading to a separation efficiency less than unity. This means that mass and heat transfers were driven by gradients of the chemical potentials and temperature. Due to these facts, the equilibrium–based models are usually inadequate and resistances to mass and heat transfer can only be considered by rate–based models in which the gas and liquid phases are balanced separately taking into consideration the mass and heat fluxes across the interface. Rigorous predictive models must regard the accelerating or inhibiting effects of chemical reactions on mass transfer and vice–versa. The non-equilibrium gas/liquid model includes an interfacial mass transfer rate where the equilibrium between phases occurs exactly at the gas/liquid interphase only. The non-equilibrium model also takes into account the flow dynamics

where the pressure drops across the packing is considered to be a function of the interstitial velocity, the physical properties and the hardware design. The column design information is then necessary, and must be specified, so that parameters such as mass transfer coefficients, interfacial areas and liquid hold-ups can be predicted. The model also requires thermodynamic and transport properties, not only for calculation of the phase equilibrium but also for calculation of the driving forces for mass and heat transfers in the reactive stripping/scrubbing column.

As conclusions, the models of previous mass transfer studies on the catalytic exchange process of hydrogen for water detritiation by reactive scrubbing relied on overall mass transfer coefficients that have been fitted to experimental data from dedicated columns [15-22]. Application of commercial software packages that carry advanced modelling methods and thermodynamic databases of prediction models for hydrogen isotopic exchange process has not been reported to our knowledge but dedicated simulation tools were developed in–house [19-23]. Herein, we present the applicability of the rigorous rate-based model of the commercial package Aspen plus Custom Modeler (AspenTech, 2013), as a promising tool to investigate the coupling of mass and heat transports, specific features of the reaction mixture and the synergic impact on isotope separation of the catalytic exchange process in a reactive stripping column. Taking advantage of extensive experimental results in literature on hydrogen isotopic exchange by stripping/scrubbing processing, this work presents the experimental results of chemical kinetics of the gaseous catalytic exchange, the results of modelling of reactive stripping process, including effects of significant design and operating parameters on the column performance. The methodology used is as follows: (1) the gaseous phase catalytic exchange is carried out independently and in the absence of the scrubbing process using a wet-proofed platinum/SDBC resin catalyst. A kinetic model for the overall rate of exchange process is developed, and relevant parameters are estimated based on data generated using deuterium. (2) The missing physical properties of deuterium and tritium isotopologues for hydrogen and water are predicted by using existing thermodynamic models, geometric mean interpolation and linear correlation of the critical properties. (3) The effects of transport and reaction kinetics on the transfer of deuterium between the liquid and gaseous phases is investigated by three types of models based on coupling as shown in Fig.1: the chemical equilibrium and the bulk gas/liquid physical equilibrium (CEPE) controlled model (Fig.1 (a)), the chemical kinetics and the bulk gas/liquid physical equilibrium (CKPE) controlled model (Fig.1 (b)) and the chemical kinetics and the rate-based gas/liquid non-equilibrium (CKRN-E) controlled model (Fig.1 (c)). The results are discussed and validated by comparison with published data and a sensitivity analysis is extended to tritium separation.

2. Materials and methods

The kinetics tests were carried out by following the kinetics of transfer of deuterium from water vapour to hydrogen gas (i.e. the reverse reaction of Eq. 1) as it is more affordable to feed the CECE column with deuterated liquid water than deuterated hydrogen gas. Directed by experiments illustrated in previous studies on fluid flow in the isotopic exchange process, the resistance to external mass transport was reduced by setting the minimum flowrate of H_2O_V and H_2 to 300 cm^3/min and the internal mass transport inside catalyst was reduced by using particles as small as 0.08–0.10 mm [24]. The kinetic tests of the catalytic exchange were carried out in a packed bed reactor as shown in Fig.2. The tube was made of fused quartz with a 12 mm internal diameter and filled with 0.75 g of hydrophobic Pt/SDBC resin (average pore size 110–175 Å, surface area 900 m^2 g^{-1} and 2% impregnated platinum) as reported by Nic An tSoir et al. [25]. The catalytic system was initially reduced under 25 mol. % of H_2 and then purged with nitrogen. Typically, a D_2O_V composition of 12.0 mol. % (relative humidity (RH) of 60.1%) was introduced at atmospheric pressure by bubbling a mixture of H_2 (20 mol. % in N_2) at 338 cm^3/min and temperature of 333 K using a controlled evaporator mixer (Bronkhorst). All pre- and post-packed tube pipes were insulated and heated to the operating temperature. Thermocouples were placed in front and behind the packed bed. In addition, a humidity sensor (Exo Terra Digital Hygrometer, accuracy 2% at RH

> 10%) was placed at the exit of the experimental setup. The output products were measured using a Pfeiffer Omistar GSD O mass spectrometer equipped with a quadrupole analyser.

3. Results

3.1. Kinetic study and composition trends

The development of kinetic study of isotopic exchange was carried out because the rate of kinetic model impacts the driving forces of concentrations and temperature that are responsible of mass transfer rates in the reactive stripping process. Two approaches are available in literature on the kinetics of the isotopic exchange: the first uses a lumping model where trends of gathered atomic concentration of deuterium per phase (gas or vapour) is considered while the second proceeds with trends of concentration of each species in the gaseous phase mixture regardless the nature of the phase. Herein, the later approach was considered and investigated under gaseous/vapour operations only. Most of the studies in literature presented kinetic models that consider reaction 1 only. Associated side reactions and intermediate isotopologues were however demonstrated in our previous works [10, 11 and 24] and were validated by a recent study by Roland et al. [26]. Kawakami et al. [27] and Sagert and Pouteau [28] studied the kinetics of the gas-phase exchange reaction (reaction 1) with the deuterium isotopologue over the supported platinum catalysts and proposed a reaction mechanism based on the Langmuir−Hinshelwood approach. Kumar et al. [17] investigated the impact of external and internal mass transports on the intrinsic kinetics of catalytic exchange in absence of the gas/liquid scrubbing. Strong pore diffusion was observed, leading to internal effectiveness factors ranging from 13 to 20 %, while the external mass transfer resistance was negligible at the operated conditions. Roland et al. [26] reported rate coefficients for the isotope exchange reactions between deuterium gas and water vapour taking place at the surface of a stainless steel vessel. Time transients of D_2O_V and HDO_V, produced via isotope exchange reactions in the mixture of D_2, H_2, and D_2O_V, H_2O_V, HD and HDO_V, were measured. The results were adequately represented by the kinetic model in the form of coupled rate equations and the validity of the model was reported to be limited to low pressure environments and large gas (D_2) to water ratios. In a previous work, we used the gas phase hydrogen catalytic exchange to visualize mass, heat and fluid flow distributions in a gas-solid packed bed reactor. The packed bed was filled with Pt/SDBC. The derived transient changes of H_2O_V, HDO_V and temperature of the vapour phase hydrogen isotopic exchange reaction, between heavy water vapour (D_2O_V) and hydrogen gas, were described by 3D distributions inside and at the exit of a packed bed reactor [24,25]. Herein, the kinetics of reaction (1) were investigated by observing the evolution of the six molecular species of hydrogen gas (H_2, HD and D_2) and water vapour (H_2O_V, D_2O_V and HDO_V) involved in the overall catalytic process. Although a total of six reactions between the water vapour isotopes and hydrogen have been reported by Roland et al.[26], only three reactions were, in fact, independent as confirmed by Roland et al. [26]. Two of these reactions were determined to be under kinetic control. Fig. 3 (a) shows transient composition profiles of the water vapour (H_2O_V) isotopologues (D_2O_V and HDO_V) and hydrogen gas isotopologues (HD and D_2) by using inlet compositions of D_2O_V and H_2 of 12.0 and 25.0 mol % in N_2, respectively, and temperature of 333 K. The steady-state compositions were achieved after 50 minutes. It is interesting to see that compositions of HD and HDO compounds followed similar trends, while amounts of D_2 were negligible, demonstrating a similar operating mechanism for the gaseous and vapour components. The production of water, even in small amounts (~ 2%), demonstrates that its production occurs via D_2 release. Deuterium was released from D_2O_V by single and double de-deuteriations: the first into HDO_V and HD, and the second into H_2O_V and D_2. D_2 compound was completely consumed while HD was partly consumed by H_2O_V into HDO_V. Therefore, the model of Roland et al. [26] is still valid but reduced to three reactions (i.e. reactions 4–6) where reactions 4 and 6 were assumed to be under kinetic control and reaction 5 under a quasi-equilibrium state [26].

$$H_2 + D_2O_V \Leftrightarrow D_2 + H_2O_V \quad (4)$$

$H_2 + D_2 \Longleftrightarrow 2HD$ (5)

$HD + H_2O_V \Longleftrightarrow H_2 + HDO_V$ (6)
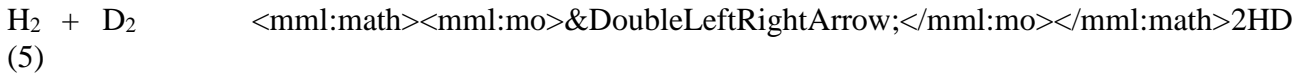
The sum of these reactions (the reverse reaction of Eq. 1) leads to Eqs. 7.1 and 7.2.

$H_2 + D_2O_V \Longleftrightarrow HD + HDO_V$ (7.1)

$H_2 + D_2O_V \Longleftrightarrow D_2 + H_2O_V$ (7.2)

The kinetics of gas phase catalytic exchange have been generally modelled by the surface Langmuir−Hinshelwood (LH), Eley−Rideal (ER) or linear adsorption mechanisms where the hydrogen and water molecules are dissociatively adsorbed at common or separate active sites. The high dilution of deuterium in water and hydrogen gas, along with relevant high adsorption capacities, led the rate for each surface reaction to be assumed of the first-order in coverage for each species [17]. The reaction rates, r_j, for reactions 4 and 6 are illustrated by Eqs. 8 and 9, respectively.

$$r_4 = k_{r,4}\left(\frac{y_{D_2O_V}}{y_{H_2O_V}} - \frac{1}{K_{eq_4}}\frac{y_{D_2}}{y_{H_2}}\right)$$ (8)

$$r_6 = k_{r,6}\left(\frac{y_{HD}}{y_{H_2}} - \frac{1}{K_{eq_6}}\frac{y_{HDO_V}}{y_{H_2O_V}}\right)$$ (9)

Where y_i is the mole fraction of species i in the gaseous phase (i.e. hydrogen and vapours). The quasi-equilibrium state of reaction 5 is taken into consideration by means of the mass action law:

$$K_{eq_5} = \frac{y_{HD}^2}{y_{D_2}y_{H_2}}$$ (10)

For the three reactions 4-6, the equilibrium constants K_i were obtained from Gibbs free-energy which was predicted in section 3.2.1 on property estimations and these equilibrium constants were compared with those reported by Yamanishi et al. [20], as shown in Fig.3 (b).

A plug flow packed bed gas–solid model was developed where dispersions inside the packing were assumed negligible. The minimization of the sum of squares of residuals was performed by the non-linear least squares method, using the Marquardt method to adjust the kinetic parameters. The validity of the kinetic model was verified by calculating the relative deviation between experimental data and predicted results from the kinetic model. Data fittings are illustrated by Fig.3 (e) for catalytic tests performed at various residence times and temperatures. The model clearly captures the trends in the data and fits the steady-state variations of the gas compositions well. The Arrhenius plots of the two kinetic constants $k_{r,4}$ and $k_{r,6}$ are given in Fig.3 (e) along with the

activation energies and pre-exponential factors of each reaction. The activation energy for the hydrogen exchange from the D_2O_V reaction is slightly higher than that of HDO. This explains why the formation of HDO_V/HD is so prominent, accounting for the majority of products at the end of each reaction. The activation energy values are within the range of reported values [41, 17], taking into account the weakening effect of platinum on hydrogen interactions due to the polarization by the SDBC resin. Figures 3 (c) and (d) confirm that HD and H_2O_V, as intermediate component in the reaction mechanism (Eqs. 4–6), present the highest compositions of HD at low conversions of D_2O_V while HDO_V production increased constantly at high conversions. This result clearly anticipates the potential merit of using a gas/liquid counter-current flow of D_2O_L and H_2 in an LPCE column, in which D_2O_V is maximized along the column, and thus would maintain a high production of HD and low conversion to condensable components (H_2O_V and HDO_V) as illustrated in the following section on the reactive stripping process by the equilibrium and non-equilibrium controlled models.

3.2. Effect of mass transfer rate on the separation efficiency of reactive stripping process

The application of the kinetic model of section 3.1 to the reactive stripping of deuterium from liquid water was validated by comparison with experimental data from literature. The reactive stripping extends the vapour/liquid phase exchange (Eq. 2) of D_2O_L to the products HDO_V and H_2O_V of the gaseous catalytic exchange (Eqs. 7.1 and 7.2, respectively)

$$HDO_V + D_2O_L \Leftrightarrow HDO_L + D_2O_V \qquad (11.1)$$
$$H_2O_V + D_2O_L \Leftrightarrow H_2O_L + D_2O_V \qquad (11.2)$$

Summation of Eqs. 7.1, 7.2, 12.1 and 12.2 leads to the overall Eqs. 12.1 and 12.2.

$$H_2 + D_2O_L \Leftrightarrow HDO_L + HD \qquad (12.1)$$
$$H_2 + D_2O_L \Leftrightarrow H_2O_L + D_2 \qquad (12.2)$$

The overall exchange rate constant of isotopic exchange between hydrogen gas and liquid water (Eqs. 12.1 and 12.2) was assessed by averaging the overall exchange rate of deuterium composition along the column height and illustrated by Eq. 14.1 and eq. 14.2 [2].

At a given height of a column of height Z, the exchange rate is expressed by Eq. 13.

$$G\,d\,y = K_{g,overall}\,\left(y_{D,eq} - y_D\right)\,d\,Z$$

 </mml:mtext><mml:mtext> </mml:mtext><mml:mtext> </mml:mtext><mml:mtext> </mml:mtext><mml:mtext> </mml:mtext><mml:mtext> </mml:mtext><mml:mtext> </mml:mtext><mml:mtext> </mml:mtext><mml:mtext> </mml:mtext><mml:mtext> </mml:mtext><mml:mtext> </mml:mtext><mml:mtext> </mml:mtext><mml:mtext> </mml:mtext><mml:mtext> </mml:mtext><mml:mtext> </mml:mtext><mml:mtext> </mml:mtext><mml:mtext> </mml:mtext><mml:mtext> </mml:mtext><mml:mtext> </mml:mtext><mml:mtext> </mml:mtext><mml:mtext> </mml:mtext><mml:mtext> </mml:mtext><mml:mtext> </mml:mtext><mml:mtext> </mml:mtext><mml:mtext> </mml:mtext><mml:mtext> </mml:mtext><mml:mtext> </mml:mtext><mml:mtext> </mml:mtext><mml:mtext> </mml:mtext><mml:mtext> </mml:mtext><mml:mtext> </mml:mtext><mml:mtext> </mml:mtext><mml:mtext> </mml:mtext><mml:mtext> </mml:mtext><mml:mtext> </mml:mtext><mml:mtext> </mml:mtext><mml:mtext> </mml:mtext><mml:mtext> </mml:mtext><mml:mtext> </mml:mtext><mml:mtext> </mml:mtext><mml:mtext> </mml:mtext><mml:mtext> </mml:mtext><mml:mtext> </mml:mtext><mml:mtext> </mml:mtext><mml:mtext> </mml:mtext><mml:mtext> </mml:mtext><mml:mtext> </mml:mtext><mml:mtext> </mml:mtext><mml:mtext> </mml:mtext><mml:mtext> </mml:mtext><mml:mtext> </mml:mtext><mml:mtext> </mml:mtext><mml:mtext> </mml:mtext><mml:mtext> </mml:mtext><mml:mtext> </mml:mtext><mml:mtext> </mml:mtext><mml:mtext> </mml:mtext><mml:mtext> </mml:mtext><mml:mtext> </mml:mtext><mml:mtext> </mml:mtext><mml:mtext> </mml:mtext><mml:mtext> </mml:mtext><mml:mtext> </mml:mtext><mml:mtext> </mml:mtext><mml:mtext> </mml:mtext><mml:mtext> </mml:mtext><mml:mtext> </mml:mtext><mml:mtext> </mml:mtext><mml:mtext> </mml:mtext><mml:mtext> </mml:mtext><mml:mtext> </mml:mtext><mml:mtext> </mml:mtext><mml:mtext> </mml:mtext><mml:mtext> </mml:mtext><mml:mtext> </mml:mtext><mml:mtext> </mml:mtext><mml:mtext> </mml:mtext><mml:mtext> </mml:mtext><mml:mtext> </mml:mtext><mml:mtext> </mml:mtext><mml:mtext> </mml:mtext><mml:mtext> </mml:mtext><mml:mtext> </mml:mtext><mml:mtext> </mml:mtext><mml:mtext> </mml:mtext><mml:mtext> </mml:mtext><mml:mtext> </mml:mtext><mml:mtext> </mml:mtext><mml:mtext> </mml:mtext><mml:mfenced open="(" close=")"><mml:mrow><mml:mn>13</mml:mn></mml:mrow></mml:mfenced></mml:mrow></mml:math>

Considering the dilution of deuterium in both phases, integration of eq. 13 throughout the entire column leads to Eq. 14.1.

$$K_{g,overall} = \frac{G^{'}}{h_F} \frac{\left(y_{D,out} - y_{D,in}\right)}{\left(y_{D,eq} - y_D\right)_{out} - \left(y_{D,eq} - y_D\right)_{in}} \ln \frac{\left(y_{D,eq} - y_D\right)_{out}}{\left(y_{D,eq} - y_D\right)_{in}}$$

(14.1)

$$y_D^{'} = \frac{y_{D_2} + \frac{1}{2} y_{HD}}{y_{H_2}}$$

(14.2)

Where y'_D represent the atom fraction of deuterium in hydrogen gas, h_F is the height of the full packing, $K_{g,overall}$ is the overall exchange rate constant based on the gas phase and y_{eq} is the composition of deuterium that would be in equilibrium with the deuterium composition of the water at that same height in the column.

A universal equilibrium model for a maximum separation efficiency and a non-equilibrium model based on a description of a single stage section representing a packing segment of a column were developed. Unlike the universal equilibrium model, the non-equilibrium model required the gas and liquid phases to be balanced separately. Both the equilibrium–based model and the rate–based model, denoted RadFrac and RateFrac modules, respectively, in the Aspen Plus process software, were used to simulate the hydrogen exchange process. The equilibrium model, which assumes thermodynamic equilibrium between bulk gas and liquid phases of reaction 2 in the column, did not require setting of the packing properties, while in the rate–based model, the separation process was treated as a heat and mass transfer process and was assumed that the equilibrium only exists at the gas/liquid interface. The mass– and heat–transfer resistances were considered according to the film theory, by directly accounting for interfacial fluxes, the film model equations and associated flow dynamics. Both models were combined with the relevant reactions and missing physical properties of single components as well as relevant mixtures. The equilibrium model was used to estimate the key operating parameters for maximum separation efficiency of deuterium and then the model was extended to the rate–based model.

3.2.1. Estimation of missing physical properties

Accurate values of thermo-physical properties are needed for the equilibrium and rate–based simulations. Despite their usefulness, measurements of the thermodynamic and transport properties of hydrogen isotopes in both hydrogen (HD, D_2, HT, DT and T_2) and hydrogen oxide (HDO, D_2O, HDO, DTO and T_2O) forms, and the effects of operating pressure and temperature on these parameters, are scarce in open literature, particularly for tritium isotopologues [29]. In the last 25 years, few thermodynamic property studies have been conducted on deuterium. An equation of state for tritium is not available in the literature and experimental measurements on tritium are rather rare. Souers [30] published a review on the properties of cryogenic hydrogen and the estimated physical and chemical properties of deuterium and tritium. Since this last analysis, there have been great advances in computer technologies and equation fitting techniques, implying a need for an updated property review [29]. In addition, available database on properties of aforementioned components is limited and conspicuously incomplete in commercial process simulation packages. This is important for modelling the hydrogen isotopic exchange since unlike the isotopes of other elements, the relatively large mass differences between H, D, and T cause appreciable differences in the properties of their compounds, and even sometimes in the properties of relevant allotropes such as the ortho- and para- forms of hydrogen gas [29].

Herein, it is not intended to investigate in detail the properties of deuterium and tritium, but instead we aimed to contribute to an open database for these isotopes (D, T), in both hydrogen gas and water forms, to be used for the isotopic exchange process. This database, as illustrated in the supporting document S1, was added to the property set package of Aspen Plus by using experimental data available in literature or predicted by using (1) existing thermodynamic models, (2) interpolation using the geometric mean of well-known data of analogous isotopologues [31] and (3) linear correlation of the critical properties (critical pressure, critical temperature and critical volume), Pitzer's acentric factor and the corresponding–states principle [32-37]. The results are illustrated in Tables S1.1 and S1.2 and Figures S1 (a-e) of the supporting document S1. The property models for each component are defined in Tables S1.1 and S1.2. Figures S1 (a) and (b) which show trends with temperatures of vapour pressure and enthalpy predicted by the Soave-Redlich-Kwong (SRK) equation of state of both water and hydrogen forms of deuterium isotopologues (D_2, HD, D_2O_L and HDO_L) and tritium isotopologues (T_2, HT, T_2O_L and HDO_L). These results are in agreement with those given in the steam and hydrogen gas tables by Richardson et al. [29]. Other thermodynamic and transport properties of deuterium isotopologues, and their

changes with temperature, were fitted to well-known literature models: dynamic viscosity using the Design Institute for Physical Properties (DIPPR) model and validated by data reported by Hill from Richardson et al.[29]; thermal conductivity using DIPPR model and validated by data from Richardson et al.[29] and Matsunaga [38]; surface tension using Crabtree and Siman-Tov's model; and binary diffusivity using Wilke-Chang's model for liquid isotopologues and Chapman-Enskog-Wilke-Lee's model for gas isotopologues and validated using Kumar's results [17]. The trends of these physical properties are presented in Fig.S1 (b-d).

As previously discussed, the thermodynamic and transport properties of tritium isotopologues are limited in open literature as they are experimentally difficult, expensive and tedious to evaluate. We proceeded therefore with Friedman's model which validates a linear trend of physical properties of analogous isotopologues along with the root of molecular weights [39]. The results achieved on deuterium isotopologues were therefore extended to each three isotopologues in hydrogen gas and water forms of tritium by using the plot of physical property versus the reciprocal of the square root of their molecular weights. Figures S1 (e_1) and (e_2) shows profiles of critical properties, boiling point and molar volumes for both H_2O and H_2 isotopologues, respectively, and clearly demonstrate averaged standard deviations of 2.5 and 2.1%, respectively and a good fit with the Friedman model. Extension to tritium–based isotopologues for vapour pressure, molar volumes, enthalpy, Gibbs free energy, viscosity and surface tension were added to Fig.S1 (a–d). It is interesting to note the formation of non-ideal vapour isotopologue mixtures and negative deviation from Raoult's model, particularly at low concentrations of T_2O_V and D_2O_V and low temperatures (Fig.S1 (d)). The presence of the intermediates HTO_V and HDO_V tends to promote non-ideality. The impact of hydrogen bonds at low temperatures along with the vapour pressure of HDO and HTO_V of values which are different from the arithmetic mean of H_2O_V/D_2O_V and H_2O_V/T_2O_V pairs, respectively, might be responsible for such positive deviations [39].

3.2.2. Equilibrium model

The equilibrium model was first investigated as it does not require detailed information on properties of both hydrophobic catalytic packing and hydrophilic inert packing but requires information on thermodynamic properties of the physical and chemical equilibrium boundaries. The equilibrium model, which relies on assumption of ideal mixing between the liquid and the gaseous phases, would anticipate, according to Eq. 12, the highest separation factor $Sep_{D,eq}$ of deuterium relevant to hydrogen isotopologues.

$$Sep_{D,eq} = \frac{x'_{D,eq}\left(1 - y'_{D,eq}\right)}{\left(1 - x'_{D,eq}\right)y'_{D,eq}}$$

(15.1)

</mml:mo><mml:mfrac><mml:mrow><mml:msub><mml:mi>y</mml:mi><mml:msub><mml:mi>D</mml:mi><mml:mn>2</mml:mn></mml:msub><mml:mi>O</mml:mi><mml:mo>,</mml:mo><mml:mi>e</mml:mi><mml:mi>q</mml:mi></mml:mrow></mml:msub><mml:mo>+</mml:mo><mml:mfrac><mml:mn>1</mml:mn><mml:mn>2</mml:mn></mml:mfrac><mml:msub><mml:mi>y</mml:mi><mml:mrow><mml:mi>H</mml:mi><mml:mi>D</mml:mi><mml:mi>O</mml:mi><mml:mo>,</mml:mo><mml:mi>e</mml:mi><mml:mi>q</mml:mi></mml:mrow></mml:msub></mml:mrow><mml:mrow><mml:msub><mml:mi>y</mml:mi><mml:mrow><mml:mi>H</mml:mi><mml:mn>2</mml:mn></mml:msub><mml:mi>O</mml:mi><mml:mo>,</mml:mo><mml:mi>e</mml:mi><mml:mi>q</mml:mi></mml:mrow></mml:msub></mml:mrow></mml:mfrac></mml:mrow></mml:math>   (15.2)

Where

<mml:math><mml:mrow><mml:msubsup><mml:mi>x</mml:mi><mml:mrow><mml:mi>D</mml:mi><mml:mo>,</mml:mo><mml:mi>e</mml:mi><mml:mi>q</mml:mi></mml:mrow><mml:mo>'</mml:mo></mml:msubsup></mml:mrow></mml:math>   and <mml:math><mml:mrow><mml:msubsup><mml:mi>y</mml:mi><mml:mrow><mml:mi>D</mml:mi><mml:mo>,</mml:mo><mml:mi>e</mml:mi><mml:mi>q</mml:mi></mml:mrow><mml:mo>'</mml:mo></mml:msubsup></mml:mrow></mml:math> represent the atom fractions of deuterium in the liquid water and hydrogen phases, respectively, at equilibrium conditions.

3.2.2.1. Model development

The phase equilibrium model (CEPE), commonly known as MESH (Material balance, vapour–liquid equilibrium equations, mole fraction summations, and heat balance), along with the gas phase hydrogen catalytic exchange reaction (as expressed by Eqs. (4-6)) was used. Several assumptions have been made for formulating and solving the model equations: (1) equilibrium controlled reactions, (2) equilibrium controlled mass transfer between bulk gas and liquid phases and (3) negligible flow dispersion and pressure drops in the column.

The MESH model for steady-state operations at the jth theoretical stage is given by Eqs. 16.1-16.4, where the index j counts downwards.

☐ Mass balance

$$L'_{j-1}x_{i,j-1} - L'_j x_{i,j} + G'_{j+1}y_{i,j+1} - G'_j y_{i,j} + r_{i,j}m_{c,j} = 0 \qquad (16.1)$$

☐ Energy balance

$$L'_{j-1}h_{j-1} - L'_j h_j + G'_{j+1}H_{j+1} - G'_j H_j = 0 \qquad (16.2)$$

Where, i=1-6 (number of components), j=1-N (number of stages) and $m_{c,j}$ is catalyst load at stage j. The heat associated with the process was assumed to be driven by liquid H and vapour/gas h enthalpies which were estimated in section 3.2.1 and shown in Fig.S1 (b). L' and G' are the flow rates of liquid and gas phase, respectively and i is the reactive component. The reaction kinetic rates $r_{i,j}$ were set to zero for the CEPE model and to Eqs. 7-9 for CKPE model.

☐ Equilibrium between bulk phases

A good mixing between the phases is assumed between leaving streams at each stage, leading to equilibrium assumption between bulk phases as illustrated by Eq. 16.3.

<mml:math><mml:mrow><mml:msubsup><mml:mi>y</mml:mi><mml:mrow><mml:mi>i</mml:mi><mml:mo>,</mml:mo><mml:mi>j</mml:mi></mml:mrow><mml:mtext> </mml:mtext></mml:msubsup><mml:mo>−</mml:mo><mml:msub><mml:mi>K</mml:mi><mml:mrow><mml:mi>i</mml:mi><mml:mo>,</mml:mo><mml:mi>j</mml:mi></mml:mrow></mml:msub><mml:msubsup><mml:mi>x</mml:mi><mml:mrow><mml:mi>i</mml:mi><mml:mo>,</mml:mo><mml:mi>j</mml:mi></mml:mrow><mml:mtext> </mml:mtext></mml:msubsup><mml:mo>=</mml:mo><mml:mn>0</mml:mn></mml:mrow></mml:math>   (16.3)

The gas/liquid equilibrium constant K values of H_2O, HDO, D_2O, HTO and T_2O were calculated from non-ideal gas/liquid fugacity equilibrium models where Antoine model and NRTL model were used for the saturated vapour pressures and fugacity coefficients, respectively.

☐ Summations

$$\sum_{i=1}^{N} x_{ij} = 1, \ \sum_{i=1}^{N} y_{ij} = 1 \qquad (16.4)$$

3.2.2.2. Model validation

The base case of the reactive stripping model was developed in accordance with the experimental run conditions and modelling provided by Ye et al. [21] who investigated the steady-state catalytic exchange of deuterium between HDO and water. As no data on kinetics were reported, we assume that the catalytic exchange (reaction 1) and gas/liquid scrubbing (reaction 2) under control of the chemical equilibrium and the bulk phase equilibrium, respectively, that is, the vapour leaving any stage was in physical equilibrium with the liquid at that stage, leading to maximum separation efficiency. The influence of the temperature, pressure, vapour to liquid flow ratios and catalyst loading on the distribution of deuterium at the top of the column was investigated. Thus, the stripping column was simulated by assuming chemical equilibrium controlled conditions of the reverse reaction 1, which was expressed by reaction mechanism of Eqs. 4–6, and by assuming the wet scrubbing (reaction 2) takes place under gas/liquid bulk phase equilibrium or negligible mass/heat transfer control. A mixed deuterium–enriched water of 0.2 mol % and a high–purity natural hydrogen gas were counter-currently passed though the column. Typical operating conditions were run under a molar ratio of hydrogen gas to water flowrate of one, flow rate of H_2O_L of 3.5 mol/h, number of theoretical stages in the column of 5, and operated at atmospheric total pressure and temperature of 323 K. In order to maintain isothermal operations along the axial profile of the column and in absence of a heating jacket, a reboiler was added at the bottom of the column as a humidifier. The value of the reboiler heat duty for each run was not predicted but tuned until a constant profile of the desired temperature along the column height was achieved. The set of mass balance Eqs. 16.1–16.4 was computed by using the embedded Newton- Raphson's method based solver in Aspen plus. This method required setting of the initial values of temperatures and flowrates which were obtained from similar process and operations of stripping process without the catalytic exchange. The computation of this later allowed solutions with no convergence difficulty. The solutions by the Newton-Raphson method however, needed large computation efforts for the numerical evaluation of the element of the Jacobian matrix and calculation of its inverse matrix when the reactive stripping was added. This was caused by the small compositions of deuterium isotope, resulting in the minimization of the residuals to be more sensitive to such small amounts than the large compositions of water and hydrogen, and thus to inadequate stability in achieving convergence.

3.2.2.2.1 Effects of temperature and pressure

For deuterium removal from liquid water, the simulation was conducted at temperatures ranging between 293.3 and 353.3 K. The deuterium in D_2O_L was converted into HDO_V, D_2 and HD as shown by Eqs. 4–6. The top column released a non-condensable hydrogen gas mixture (i.e. H_2, HD and D_2) and a condensable water vapour mixture (i.e. H_2O_V, HDO_V and D_2O_V). Since the vapour phase is commonly condensed and recycled back to the column, the separation of deuterium from liquid water relies on its presence in the hydrogen gas mixture (D_2, HD in H_2) only. The composition of the condensable vapour phase (i.e. D_2O_V and $HDO_{V)}$ and relevant atom fraction of deuterium in the vapour phase, $x^{'}_D$ as well as the composition of hydrogen phase (i.e. D_2 and HD) and relevant atom fraction of deuterium in hydrogen phase, $y^{'}_D$, at the top exit are shown in Fig.4 (a). Similar to the results reported by Ye et al. [21]. At atmospheric pressure the concentration of deuterium in the hydrogen gas increased with temperature until about 348 K and then decreased owing to increased presence of H_2O_V at high temperatures, promoted by the higher relative volatility of H_2O_V compared with HDO_V, as illustrated in Fig.2 (a), leading to more condensation of

HDO$_V$ than H$_2$O$_V$, favouring a shift of the chemical equilibrium of reaction 12.1 and 12.2 towards H$_2$O$_V$ production. The trends of increase or decrease in HDO$_V$ production was thus dominated by relevance of chemical equilibrium of reactions 4-6 and reaction 12. The CEPE model was first validated by the separation factor $Sep_{D,e}$ of deuterium from water to hydrogen gas at as computed by Eq. 15.1. The values of separation factor at atmospheric pressure is within a reasonable agreement (i.e. deviation of 1.2 %) with the model proposed by Rolston et al. [40].

The effect of total pressure was investigated by the CEPE model while a negligible deactivation by pore condensation of water was assumed. Increasing the total pressure, as suggested by Sugiyama et al. [4], would maintain high H$_2$O$_L$ levels in the liquid phase at high temperatures. This is confirmed by Fig.4 (a), which validates that reducing the pressure leads to increased proportion of H$_2$O$_V$ and a reduced concentration of deuterium in the hydrogen gas. Thus, operating at high pressures promoted the presence of deuterium, mainly in HD form, in the hydrogen gas at reduced H$_2$O$_V$ and D$_2$O$_V$ compositions but extending to temperatures beyond maximum HD compositions favoured relevance of reaction 12 over reactions 4-6 at reduced HD and HDO$_V$ productions.

3.2.2.2.2 Effect of feed flow ratio of hydrogen to water (G'/L')

Since operations were carried out under chemical and physical equilibrium of reactions 2 and 4-6, changing the feed flowrate ratio of H$_2$ to H$_2$O$_L$ affected exclusively the equilibrium compositions of reactions 2 and 4-6. Trends of HD again has shown maximum values with operating temperatures for each value of G'/L' ratio. These temperature for maximum HD production were approximately 343, 323 and 293 K at G'/L' values of 1, 2 and 4, respectively, as shown in Fig.4 (b). High G'/L' ratios produced less pure deuterium in the hydrogen phase due to higher loads of hydrogen feed. Other potential advantages of increasing the feed rate of hydrogen, such as mass transfer rates and flow dynamics in the packing, were not accessible owing to assumption of bulk gas/liquid equilibrium operations.

3.2.2.2.3. Effect of number of stages

Alternatively, rather than reducing gas flowrates, increasing the number of stages or packing height would instead present similar trends of deuterium separation, as observed in Fig.4 (c), which shows the effect of the number of stages (N = 2–8) on the concentration of deuterium at the top of the column. A set of simulations were run to determine the effect of packing height on deuterium capture at a constant value of unity for G'/L' ratio. It is clear that the deuterium capture increased with increasing column height, up to a packing height of five theoretical stages and then remained reasonably unchanged thereafter. This may be due to attainment of maximum separation efficiency which was driven the chemical equilibrium compositions of both reactions 12.1-12.2 and 4-6.

3.2.2.2.4. Effect of mass of catalyst

Under chemical kinetic operations, the reaction time of the catalytic exchange (Eqs. 4-6) would affect the overall gas/liquid mass transfer boundaries. Thus, the chemical kinetic module in Aspen plus was then turned on and added to the phase equilibrium module. The chemical kinetic module included chemical kinetics of reaction 4 and 6. The CKPE model is thus used instead of CEPE that has been used in sections 3.2.2.1-3.2.2.3. Fig.4 (d) shows the benefit of using the reactive stripping when compared with gaseous phase catalytic exchange only in section 3.1). Unlike the results in Fig.3 (c), which were obtained by operating the isotopic exchange under a gaseous phase only, the results of the reactive stripping process as illustrated in Fig.4 (d) shows an increase in conversion into HD gas when the mass of catalyst was increased. Increasing the mass of catalyst promoted the rate of conversion of D$_2$O$_L$ into HD gas compared with HDO$_V$ as shown in Fig.4 (d). Since the resistance to gas/liquid mass transfer was ignored in the phase equilibrium model, the amount of catalyst for HD conversion was over-predicted owing to rapid counter-current mass transfer of H$_2$O$_L$ into the hydrogen gas phase and HDO$_V$ into the liquid water phase compared with relevant chemical kinetics. At high values of catalyst mass, the conversion reached asymptotic values close to the equilibrium ones obtained in Fig.4 (a).

In addition, the composition profiles of isotopologues and corresponding reaction rates inside the column, as shown in Fig.4 (e), clearly indicates that most of the conversion into HD took place throughout the bottom part of the column (stages 4–6). Maximum values of HD composition were achieved over the packing height, justifying the role of HD as intermediate towards HDO_V production as shown in Eqs. 4-6 and the efficient condensation of this later (Eq. 11) as assumed in the CEPE model, and thus demonstrating an excess use of reactive stages when the full column is packed with reactive packing.

3.2.3. Rate–based non-equilibrium model

Assuming well defined mass transfer inside the catalyst packing, the mass transfer rate of deuterium from the liquid water to hydrogen gas phase depends on the external mass transfer, which is a function of fluid dynamics. The fluid dynamics consist of an upflowing hydrogen gas, which gets saturated with water vapour at the operating temperature and offers a holdup equivalent to the open space of the reactor while the liquid water trickles down and covers the wettable surface of both the inert and reactive packings. Thus, the mass transfer is a function of the exposed surface area of the down-flowing H_2O_L and shaped by the packing material. The overall mechanism of mass transfer herein includes, according to the two–film theory, transport of D_2O_L reactant to the liquid film interface through the down-flowing H_2O_L, diffusion of D_2O_L through the film, evaporation at surface interphase into D_2O_V, diffusion of D_2O_V in the gas film and transport in the up-flowing gas, and opposite mass transfer pathway applies to condensation of produced HDO_V, transport of D_2O_V in core of the gas phase and surface reactions in the hydrophobic reactive packing. Thus, the mass transfer is a function of the chemical kinetics, packing properties and flow dynamics (accessible surface area, wettability, holdup and pressure and temperature).

The rate–based module of Aspen plus was used as a basis for simulating the reactive stripping process of hydrogen isotopic exchange. The module combines CKRN-E models and thus is a powerful tool for the design and scale-up analysis of the hydrogen exchange process, as it has the capability of employing real reactive stripping configurations of internals, multi-component mass and heat transfer methods, actual chemical kinetic and thermodynamic models. However, this model requires good underlying models for kinetics, thermodynamics and hydrodynamics.

1.2.3.1 Model development

The CKRN-E model uses separate mass balance models for each phase along with rate of mass and heat exchanges between the gas and liquid phases. The set of mass and heat balance equations for bulk phases and interphases is illustrated in Eqs. 17.1-17.10 while the set of mass transfer equations at interphase, mixing rules of properties, correlations for mass and heat transfer coefficients and pressure drops is illustrated in Appendix A.

☐ Mass balance:

- Material balance for bulk liquid

$$L_{j-1}' x_{i,j-1} + NM_{i,j}^{L} - L_j' x_{ij} = 0 \quad (17.1)$$

- Material balance for bulk gas

$$G_{j+1}' y_{i,j+1} - N M_{i,j}^{G} + r_{ij}^{G} - G_j' y_{...}$$

$\ldots_{ij} = 0$ (17.2)

- Material balance for liquid interphase film

$$NM_{ij}^{I} = NM_{ij}^{L}$$ (17.3)

- Material balance for gas interphase film

$$NM_{ij}^{I} = NM_{ij}^{G}$$ (17.4)

Where *NM* is the rate of mass transfer between the liquid and gaseous phases

☐ Energy balance
- Energy balance for bulk liquid

$$L_{j-1}^{'}H_{j-1} + q_{j}^{L} - L_{j}^{'}H_{j} = 0$$ (17.5)

- Energy balance for bulk gas

$$G_{j+1}^{'}h_{j+1} - q_{j}^{G} - G_{j}^{'}h_{j} = 0$$ (17.6)

- Energy balance for liquid interphase film

$$q_{j}^{I} = q_{j}^{L}$$ (17.7)

- Energy balance for gas interphase film

$$q_{j}^{I} = q_{j}^{G}$$ (17.8)

Where *q* is the heat transfer associated with the mass transfer between the phases

☐ Phases equilibrium at gas/liquid interphase

$$y_{ij}^{I} - K_{ij}x_{ij}^{I} = 0$$ (17.9)

☐ Summations

$$\sum_{i=1}^{N} x_{ij} = 1,\; \; \sum_{i=1}^{N} y_{ij} = 1,\; \sum_{i=1}^{N} x_{ij}^{I} = 1\; ,\; \;$$

><mml:munderover><mml:mo>∑</mml:mo><mml:mrow><mml:mi>i</mml:mi><mml:mo>=</mml:mo><mml:mn>1</mml:mn></mml:mrow><mml:mi>N</mml:mi></mml:munderover><mml:mrow><mml:msubsup><mml:mi>y</mml:mi><mml:mrow><mml:mi>i</mml:mi><mml:mi>j</mml:mi></mml:mrow><mml:mi>I</mml:mi></mml:msubsup></mml:mrow><mml:mo>=</mml:mo><mml:mn>1</mml:mn></mml:mrow></mml:math>   (17.10)

3.2.3.2. Model validation

The thermodynamic model, physicochemical properties and chemical kinetic modules package were similar to those used in the equilibrium model, whereas the mass and heat transfer models were switched to the mass and heat transfer rate–based model. This model included a transport rating module for the column used. The column rating allowed access to flow dynamic properties (i.e. liquid holdup, maximum liquid velocity before flooding and pressure drops) as well as to mass and heat transfer properties (i.e. interfacial area, heat and mass transfer coefficients, composition and temperature at gas/liquid interface and height equivalent to a theoretical plate (HETP). The rate-based model, which is based on the two film theory, included the mass and heat transfer rates between the contacting phases and was based on a detailed description of the combined diffusion and advection processes taking place in both the liquid and gaseous phases, while phase equilibrium existed at the gas and liquid interface and a relevant transfer model was used to calculate the gas/liquid phase resistances.

The ``VPLUG'' flow model (Eqs. A.1-A.10 in Appendix A) in which the bulk properties for each phase were assumed to be the same as the outlet conditions for that phase leaving that stage model, was used to calculate the bulk properties, including the reaction, energy and mass rates. Mass transfer coefficients and interfacial area were calculated using Onda's model [18] (Eqs. A.11-A.17 in Appendix A) as it is recommended for the Dixon packing used. In addition, the pressure drop model presented by Billet and Schultes [41] (Eqs. A.18-A.20 in Appendix A) was assumed applicable to the Dixon packing and the heat transfer coefficient was predicted by the Chilton and Colburn analogy [42]. The absorber heat loss was assumed negligible.

The results of Ye et al. [21] first validated this model as a means to investigate the actual separation efficiency of the mass transfer based non-equilibrium model. The reactive stripping column was set with a size of 0.025 m I.D. and 1.20 m length, resulting into five to six HETP depending on the operated flow rates used. This HETP corresponds approximately to a single section of packing inside Ye's column which was equally filled with inert hydrophilic packing and reactive hydrophobic packing. The model was validated as well with results from Kumar et al. [17] and a sensitivity analysis was then applied which utilized the packing configuration, kinetic models, gas and liquid mass transfer coefficients, and the effective interfacial area to determine the effects of different design parameters on performance of separation of deuterium into HD gas at the top of the reactive stripper.

Fig. 5 (a$_1$) shows the trends of product profiles with temperature for the combined chemical kinetics and the rate-based gas/liquid non-equilibrium model (CKRN-E) along with the two previously discussed the chemical equilibrium and the bulk gas/liquid physical equilibrium (CEPE) model and the chemical kinetics and the bulk gas/liquid physical equilibrium (CKPE) model. The profiles of deuterium in hydrogen phase, by inference HD compositions, by the rate-based model were favoured at high temperatures owing to increase of both mass transfer rates and chemical kinetic rates. These trends are similar to those observed by Ye et al. [21] and the deviations from the chemical equilibrium model are more pronounced at low temperatures where conversion into HD was not significant. At high temperatures, these deviations were about one third those observed by Ye and about one half those observed in the CKPE equilibrium model, leading to conclude that the kinetic rate model would have fit the results of Ye well if the catalyst were more active.

The results were as well compared with those from Kumar et al. [17] who simplified the hydrogen exchange process into a single reaction involving the conversion of deuterated water into HD to facilitate the use of a two-phase model, and the sensible heat transfer between phases and back

absorption of hydrogen gases by water were as well ignored. The trend of composition of deuterium at the top of column in hydrogen gas as shown in Fig.5 (a_2) shows negative deviation about 20 %, which is reasonable, considering the catalytic activity of present packing along with the errors associated with the physical properties, fluid flow model, Onda's mass transfer correlations and experimental runs.

The trends observed using the equilibrium–based model (CEPE or CKPE) were also observed in the non-equilibrium model (CKRN-E), but with a significant deviation of HD composition at the top of the column, particularly at low temperatures. The contribution of gas/liquid mass transfer limitation at low temperature is also validated by the deviation of the rate constant of the gaseous catalytic exchange (Eq. 4) from the overall gas/liquid rate constant as shown in Fig.5 (b_1) and ratio of gaseous reaction rate to gas/liquid mass transfer rate (Fig.5 (b_2)). This would demonstrate that the non-equilibrium model predicts mass transfer resistance between the gas phase and the liquid water phase, particularly the counter-current mass transfer of D_2O_L and H_2O_L mixture from the liquid to H_2 phase, and HDO_V from the gas phase to the liquid water phase.

The mass transfer at liquid/gas interphase boundary and the overall mass transfer from the H_2O_L to the catalytic packing were investigated and the model parameters, including mass transfer coefficients and relevant rates were validated by experimental tests of Kumar et al. [17]. Increasing the feed flow ratio (G'/L') of hydrogen to water at constant liquid flowrate was effective on mass transfer coefficients in the gaseous phase only (Fig.5 (c_1)) while increasing the liquid flowrate (L'/G') was relevant for both liquid and gas mass transfer coefficients (Fig.5 (c_2)), demonstrating the relevance of transport resistance inside the film on the gas phase side at present operating conditions. These values of mass transfer coefficients were in the range of those obtained by Kumar et al. [17], validating the use of Onda's model.

Unlike the equilibrium model (CKEP), where the temperature affected the chemical rate constants of reactions, saturation of hydrogen phase by water vapours (D_2O_V, HDO_V and H_2O_V) and flow enthalpies, the rate–based model ((CKRN-E) was even more sensitive to temperature due to the dependency of additional physical property parameters on temperature, including the solubility of isotopologues in water, diffusivity in both gaseous and liquid phases, viscosity, surface tension, thermal conductivity and heat capacity.

Fig. 5 (d) compares the profiles of compositions of HDO_V and HD components along the column height obtained using either the rigorous mass transfer CKRN-E model or the equilibrium CKEP model which were illustrated in Fig.4(e). Literature on experimental data of compositions profiles of deuterium inside the column is limited and the following results were validated by those obtained by Kumar et al. [17] as well as by those derived from the top or bottom of the column. The equilibrium model significantly overestimates the stripping of D_2O as well as the scrubbing of HDO, and thus provides non-reliable results, leading to lower packing heights and hence to incorrect process designs. This is contrary to the rigorous rate–based model which produced less HD and HDO_V, particularly towards the top of the column, owing to lower chemical conversion of D_2O_L with the later model. The CKRN-E model exhibited steady trends of HD and HDO compared to the curvy trends observed in CEPE and CKEP models owing to inhibited counter-current mass transfer of D_2O_L and HDO_V to the H_2 and H_2O_L phases, respectively.

3.2.4. Sensitivity analysis of the rate-based model

The sensitivity of the rate-based model to column internals and to additional presence of tritium was investigated by observing the overall chemical exchange of the reactive stripping column. The column internals affect the trickling flow, pressure drops, liquid holdup and wetting efficiency of the reactive packing. The coexistence of deuterium along with tritium affects relevant separation boundaries of each as demonstrated by the thermodynamic properties in section 3.2.1.

3.2.4.1. Effect of pressure drop

Pressure drop is an important design parameter which influences the size of the LPCE column. Significant energy savings can be achieved in the reactive stripper by using the appropriate size of

the column, (i.e. the proper height–diameter ratio). A sensitivity analysis was performed to assess the pressure drops in the reactive stripper. The pressure drop profiles were evaluated using Billet's model [41] applied to Raschig like packing as models applied to Dixon packing are not available. As illustrated in Fig.6 (a), the predictions of the rate–based model are not in agreement with the pilot data reported by Ye et al. [21], as the value herein (i.e. 17.7 Pa/m for a Dixon packing of 1.5 mm particle size, G'/L' ratio of unity, six theoretical stages and an inlet liquid flowrate of 3.5 mol/h) is about at least one fourth the values previously cited. However, a detailed knowledge of pressure drop measurement, in addition to column packing specifications including type of liquid distributors and liquid collector were missing in Ye's results, and matching our results to the measured pressure drop would not be possible. Changing the Dixon packing size from 1.5 to 6.0 mm led to a decrease in the pressure drop from 17.7 to 9.4 Pa/m. The composition profiles over the column height in Fig.6 (a) clearly show s steady decrease of HD over the column height owing to HDO_V condensation (Eq. 11.1). Even though the packing size of 1.5 produced a higher composition of HD at the bottom of the column, it exhibited a higher decrease over the column height compared with packing of 6.0 mm particle size. This result was expected since the pressure drops is known to be driven by the gaseous phase under trickling flow according to Billet and Schultes model, validating our previous finding of mass transfer control of D_2O_L and HDO_V by hydrogen gas film only.

<H4>3.2.4.2. Effect of packing configuration

The configuration of the packing was insured by mixing both hydrophilic and hydrophobic packing in a single unit, allowing both chemical reactions (reaction 1 or reactions 4-6) and gas/liquid mass transfer (reaction 2) to occur simultaneously throughout the packed bed. This configuration promoted the rate of mass transfer (reaction 2) but could deactivate, and thus inhibit, reaction (1) after long-term use, owing to the partial wetting of catalyst surfaces. Layered packing, as suggested by Sugiyama et al. [8, 43], represents another packing configuration where segregated modules that alternate catalytic packing layer and inert packing layer were designed, allowing both reactions to occur separately. This segregated arrangement allowed only the gaseous phase to flow through the catalyst packing surfaces, thus reducing potential deactivation. An arrangement of layered packing where stages 1, 3 and 5 included the catalytic packing and stages 2 and 4 included the hydrophilic Dixon packing. This arrangement of layered and inert packing was compared herein with the homogeneous arrangement assuming similar packing properties (i.e. Dixon type, size of 1.5 mm and concentration of 50% inert packing and 50% of reactive packing). As evidenced in Fig.6 (b), the homogeneous packing presented a higher HD production than the segregated packing under similar operating conditions. These results validate those obtained by Sugiyama et al. [8], where the production of HD gas was higher when homogeneous packing was employed. Thus, fresh catalysts beads would be suitable for homogeneous packing but for long-term operations of the isotopic exchange process, more investigation is needed on the rate-based model that would include the deactivation effect of catalyst.

<H4>3.2.4.3. Effect of presence of tritium

Existence of tritium along with deuterium in H_2O_L was investigated in terms of their conversions into HT and HD gases. Existing literature on kinetic studies on water detritiation processing deals however mainly with deuterium exchange while the kinetics of the gaseous catalytic exchange based on tritium are limited in open literature. Consideration of many tritium based technologies relies on prediction based on experimental data of species of close properties but operated cost–effectively and safely such as deuterium isotope [24]. However, care needs to be taken when converting data from deuterium to tritium. Fedorchenko et al. [44] investigated the gaseous phase kinetics of the catalytic exchange using tritium isotopologues and compared the rates of deuterium and tritium catalytic exchange. They reported that the effectiveness factor inside the catalyst was higher with deuterium than tritium, leading to higher resistance to diffusion with tritium. However,

the intrinsic kinetic rate of tritium was about one third higher than that observed with deuterium, leading to potentially over-estimated design features based on deuterium only.

The combined model of kinetic isotopic exchange and the gas/liquid stripping process of deuterium (Eqs. 4–6) were then extended to tritium as shown by Eqs. 16–20.

$$H_2 + T_2O_v \Leftrightarrow T_2 + H_2O_v \quad (16)$$

$$H_2 + T_2 \Leftrightarrow 2HT \quad (17)$$

$$HT + H_2O_v \Leftrightarrow H_2 + HTO_v \quad (18)$$

$$D_2 + T_2 \Leftrightarrow 2DT \quad (19)$$

$$DT + H_2O_v \Leftrightarrow H_2 + DTO_v \quad (20)$$
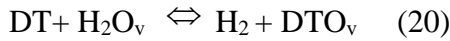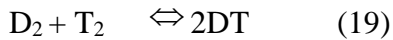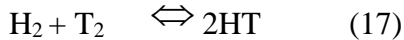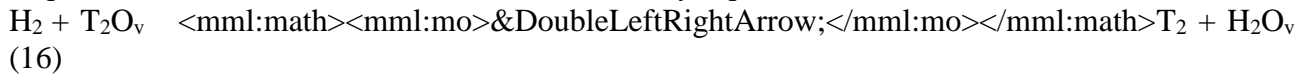
The sum of these reactions leads to the reverse reaction of Eq. 1. Perevezentsev et al.[6] observed that the mass transfer coefficient of tritium in presence of deuterium was function of concentration deuterium and gas to liquid ratio. Unlike deuterium, tritium presents extended equilibrium constant values for analogous reactions 4-6 and reactions 16–20 as well as higher enthalpy of evaporation of relevant isotopologues than those corresponding to deuterium. Herein, the equilibrium constants K_i for the five reactions 16-20 were obtained from Gibbs free energy which was predicted in section 3.2.1 on property estimations and these data were compared with those reported by Yamanishi al. [20], as shown in Fig.3 (b). In addition, Eqs. 19 and 20 clearly demonstrate impact of deuterium on overall tritium separation owing to production of HD and HDO species containing both isotopes each.

In this sensitivity analysis, effect of deuterium presence along with tritium and gas/liquid ratio on mass transfer rates was investigated. Following the kinetic trends by Fedorchenko et al. [44], the kinetic model relevant deuterium based catalytic exchange was extended to tritium. The values of kinetic constants relevant to Eqs. (16, 18 and 20) were taken as one third higher than relevant constants used for deuterium (Eqs. 4 and 6) while Eqs. 17 and 19 were again assumed under a quasi-equilibrium state [26]. The results were first validated using experimental data of Critescu et al. [16]. In this test, the H_2O_L feed at the top of the column contained composition of 2.5 mol % HDO and composition of HTO in terms of activity of 30.3 Bq/cm^3 (i.e. ~5.1 x 10^{-11} mol %) while the H_2 feed contained 0.4 mole % HD. Fig.6 (c) illustrates the results of composition profiles inside the column. The results of simulation show at the bottom of the column, lower HDO_L concentration (i.e. 1.9 mol %) and the tritium activity, (i.e. 14.5 Bq/cm^3) in the form of HTO_L and traces of DTO_L and T_2O_L) than those reached experimentally by Critescu et al. [16] (i.e. 1.5 mol % HDO and 9.3 Bq/cm^3 tritium activity). It should be noted that the operating temperature and a Dixon packing size of 3 mm allowed the column to be operated at 336 K and HETP of 0.18 m instead of 353 K and 0.65 m by Critescu et al. [16]. The higher values of HDO_L and HTO_L in the bottom of the column, although the overestimation of the mass transfer, demonstrated that the rate of kinetic model of reaction set 16-20, and by inference activity of catalyst used by Critescu, was higher than the model used for our catalyst. The mass transfer coefficients of tritium in hydrogen and water isotopologues were smaller than those of deuterium. The HEPT of about 0.18 m was found to be smaller than the one reported by Critescu but packing details and column internals were missing, making rigorous matching our results uncertain. Furthermore, the coexistence of both isotopes may have a synergetic effect of relevant separations. Unlike tritium which exists at traces levels and thus can be ignored, deuterium may reach high levels in tritiated feeds, impacting therefore the separation efficiency of tritium. The effect of deuterium content ranging from natural water to 10 mol % contents was investigated in terms of mass transfer coefficients. Fig.6 (d) illustrates trends of mass transfer coefficients K_G of both vapours and gaseous species. Increasing deuterium to values of 10 % content in the feed reduced mass coefficients by 4 to 5 % of both deuterium and tritium based species, promoting mass transfer contribution and validating relevance of species contents on diffusivity coefficients, and by inference mass transfer coefficients according to Onda's model [18]. The applicability of the rate based model of Aspen plus package was therefore successful to assess complexity of separation of isotope mixtures by reactive stripping and demonstrated relevance of

flow dynamics, process design and species loads on extend of separation efficiency from both thermodynamics and kinetic perspectives.

4. Conclusions

This work extends applicability of the equilibrium and rate–based models of commercial Aspen plus modular package to hydrogen catalytic exchange by using a reactive stripping column packed bed of Pt/SDBC resin catalyst. Compared with equilibrium model, the rate–based model, which governs the coupling of mass and heat transports and specific features of the reaction mixture of hydrogen isotope exchange, simulated more realistically the synergic effect of these on the de-deuteriation efficiency. The kinetic model confirmed a single into HD and HDO_V and double de-deuteriation into D_2 and H_2O_V when D_2O_L was used as the starting feed. The kinetic model fit the experimental data well and relevant parameters were estimated based on data generated using deuterium. The missing physical properties of deuterium and tritium isotopologues in hydrogen gas and water forms were predicted and validated within acceptable agreement with existing literature data. These physical data were needed for the bulk gas/liquid equilibrium model and even more for the rate-based non-equilibrium model. The equilibrium model (CEPE), which is independent of types of packing and catalysts but function of thermodynamic boundaries of underlying chemical reactions and gas/liquid physical exchange, allowed access to trends of maximum separation efficiency of deuterium isotope into HD that would ideally be reached under assumptions of efficient gas/liquid mixing and efficient reactive packing. The concentration of deuterium in the hydrogen gas increased with temperature and then decreased owing to increased presence of H_2O_V at high temperatures, leading to more condensation of HDO_V. Other operating parameters such as the operating pressure was effective to separation owing to reduced H_2O_V compositions, gas to liquid flow rate ratio reduced maximum separation efficiency and column height promoted local separation efficiency until a height where it remained unchanged. Under kinetic control, the phase equilibrium model (CEPE) indicated maximum values of deuterium in hydrogen over the packing height, demonstrating efficient condensation of HDO_V intermediate by the ideal mixing and limiting further de-deuteriation of this later into H_2O_V.

The rate-based model (CKRN-E) presented results close to real pilot scale data and relevant deviations of CKRN-E model from the equilibrium model allowed predictions of mass transfer rates, reactive mass transfer rates and separation efficiency of the reactive stripping column. Compared with equilibrium model, the rate–based model simulated the reactive stripping/scrubbing process more accurately, including the effects of temperature, type and properties of the packing, pressure drops and presence of tritium on the separation efficiency. The mass transfer control of D_2OL into the gaseous phase reduced overall production of HD compared with the equilibrium model. Maximum trends of HD over the packing height in the equilibrium model however were not observed in the rate-based model owing mass transfer control of HDO_V condensation, inhibiting further de-deuteriation into H_2OV and HD. The gas to liquid flow ratios demonstrated that the gas/liquid mass transfer was mainly driven by gas film side and this control was even more promoted at high temperatures, which was illustrated by overall mass transfer coefficients and isotopic exchange rate constants. The pressure drops which was mainly driven by the gaseous phase reduced the gas film resistance to mass transfer of D_2O_L into the gas phase and HDO_V into the liquid phase and thus promoted HD production for a given height of the packing only. In addition, the diluted reactive packing by an inert packing offered more separation efficiency than the layered hydrophobic/hydrophilic packing owing to liquid holdup distribution which was found more pronounced with the layered packing. Furthermore, the sensitivity of the rate-based model to the presence of tritium in a deuterated water validated over-estimated design features when deuterium is considered a reference compound for detritiation technologies owing to smaller mass transfer coefficients of tritium in hydrogen and slower kinetics leading to reduced overall isotopic exchange rates.

The originality in this work is the applicability of commercial packages such as Aspen plus modular software to catalytic isotopic exchange of hydrogen inside a reactive stripping column. Many

features of the heat and mass transfer associated with reactive stripping inside the column, including local bulk properties (compositions, temperatures, enthalpies, fluid flow, holdup, pressure drops, etc..) as well as local gas/liquid interphases properties (mass and heat transfer coefficients, compositions, temperature, mass and heat transfer rates of heat and mass transfer rates), could be computed or predicted for a rigorous design. The development of the module was demonstrated to be flexible and applicable to many similar processes including the water detritiation by reactive scrubbing processing.

ACKNOWLEDGMENTS

Appendix A

The equations below for flux demonstrate the so-called ``mixed flow model'' where outlet conditions are used for the bulk properties in each phase.
- Mass flux for liquid film

<mml:math><ThomsonDigital>WRONG STRUCTURING PLEASE CHECK THIS EQUATION??????</ThomsonDigital></mml:math>
<mml:math><mml:mrow><mml:msubsup><mml:mi>Γ</mml:mi><mml:mrow><mml:mi>i</mml:mi><mml:mo>,</mml:mo><mml:mi>k</mml:mi><mml:mo>,</mml:mo><mml:mi>j</mml:mi></mml:mrow><mml:mi>L</mml:mi></mml:msubsup><mml:mo>=</mml:mo><mml:msub><mml:mi>δ</mml:mi><mml:mrow><mml:mi>i</mml:mi><mml:mo>,</mml:mo><mml:mi>k</mml:mi></mml:mrow></mml:msub><mml:mo>+</mml:mo><mml:msub><mml:mi>x</mml:mi><mml:mrow><mml:mi>i</mml:mi><mml:mo>,</mml:mo><mml:mi>j</mml:mi></mml:mrow></mml:msub><mml:msub><mml:mrow><mml:mfenced open="" close="|"><mml:mrow><mml:mfrac><mml:mrow><mml:mo>∂</mml:mo><mml:mi>ln</mml:mi><mml:msubsup><mml:mi>ϕ</mml:mi><mml:mrow><mml:mi>i</mml:mi><mml:mi>j</mml:mi></mml:mrow><mml:mi>L</mml:mi></mml:msubsup></mml:mrow><mml:mrow><mml:mo>∂</mml:mo><mml:msub><mml:mi>x</mml:mi><mml:mrow><mml:mi>i</mml:mi></mml:mrow></mml:msub></mml:mrow></mml:mfrac></mml:mrow></mml:mfenced></mml:mrow></mml:mrow><mml:mrow><mml:msubsup><mml:mi>T</mml:mi><mml:mi>j</mml:mi><mml:mi>L</mml:mi></mml:msubsup><mml:mo>,</mml:mo><mml:msub><mml:mi>P</mml:mi><mml:mi>j</mml:mi></mml:msub><mml:mo>,</mml:mo><mml:mi>Σ</mml:mi></mml:mrow></mml:msub><mml:mtext> </mml:mtext><mml:mtext> </mml:mtext><mml:mtext> </mml:mtext><mml:mtext> </mml:mtext><mml:mtext> </mml:mtext><mml:mtext> </mml:mtext><mml:mtext> </mml:mtext><mml:mtext> </mml:mtext><mml:mtext> </mml:mtext><mml:mtext> </mml:mtext><mml:mtext> </mml:mtext><mml:mtext> </mml:mtext><mml:mtext> </mml:mtext><mml:mtext> </mml:mtext><mml:mtext> </mml:mtext><mml:mtext> </mml:mtext><mml:mtext> </mml:mtext><mml:mtext> </mml:mtext><mml:mtext> </mml:mtext><mml:mtext> </mml:mtext><mml:mtext> </mml:mtext><mml:mtext> </mml:mtext><mml:mtext> </mml:mtext><mml:mtext> </mml:mtext><mml:mtext> </mml:mtext><mml:mtext> </mml:mtext><mml:mtext> </mml:mtext><mml:mtext> </mml:mtext><mml:mtext> </mml:mtext><mml:mtext> </mml:mtext><mml:mtext> </mml:mtext><mml:mtext> </mml:mtext><mml:mtext> </mml:mtext><mml:mtext> </mml:mtext><mml:mtext> </mml:mtext><mml:mtext> </mml:mtext><mml:mtext> </mml:mtext><mml:mtext> </mml:mtext><mml:mtext> </mml:mtext><mml:mtext> </mml:mtext><mml:mtext> </mml:mtext><mml:mtext> </mml:mtext><mml:mtext> </mml:mtext><mml:mtext> </mml:mtext><mml:mtext> </mml:mtext><mml:mtext> </mml:mtext><mml:mtext> </mml:mtext><mml:mtext> </mml:mtext><mml:mtext> </mml:mtext><mml:mtext> </mml:mtext><mml:mtext> </mml:mtext><mml:mtext> </mml:mtext><mml:mtext> </mml:mtext><mml:mtext> </mml:mtext><mml:mtext> </mml:mtext><mml:mtext> </mml:mtext><mml:mtext> </mml:mtext><mml:mtext> </mml:mtext><mml:mtext> </m

ml:mtext><mml:mtext> </mml:mtext><mml:mtext> </mml:mtext><mml:mtext> </mml:mtext><mml:mtext> </mml:mtext><mml:mtext> </mml:mtext><mml:mtext> </mml:mtext><mml:mtext> </mml:mtext><mml:mtext> </mml:mtext><mml:mtext> </mml:mtext><mml:mtext> </mml:mtext><mml:mtext> </mml:mtext><mml:mtext> </mml:mtext><mml:mtext> </mml:mtext><mml:mtext> </mml:mtext><mml:mtext> </mml:mtext><mml:mtext> </mml:mtext><mml:mtext> </mml:mtext><mml:mtext> </mml:mtext><mml:mtext> </mml:mtext><mml:mtext> </mml:mtext><mml:mtext> </mml:mtext><mml:mtext> </mml:mtext><mml:mtext> </mml:mtext><mml:mtext> </mml:mtext><mml:mtext> </mml:mtext><mml:mtext> </mml:mtext><mml:mtext> </mml:mtext><mml:mtext> </mml:mtext><mml:mtext> </mml:mtext><mml:mtext> </mml:mtext><mml:mtext> </mml:mtext><mml:mtext> </mml:mtext><mml:mtext> </mml:mtext><mml:mtext> </mml:mtext><mml:mtext> </mml:mtext><mml:mtext> </mml:mtext><mml:mtext> </mml:mtext><mml:mtext> </mml:mtext><mml:mtext> </mml:mtext><mml:mtext> </mml:mtext><mml:mtext> </mml:mtext><mml:mtext> </mml:mtext><mml:mtext> </mml:mtext><mml:mtext> </mml:mtext><mml:mtext> </mml:mtext><mml:mtext> </mml:mtext><mml:mtext> </mml:mtext><mml:mtext> </mml:mtext><mml:mtext> </mml:mtext><mml:mtext> </mml:mtext><mml:mtext> </mml:mtext><mml:mtext> </mml:mtext><mml:mtext> </mml:mtext><mml:mtext> </mml:mtext><mml:mtext> </mml:mtext><mml:mtext> </mml:mtext><mml:mtext> </mml:mtext><mml:mtext> </mml:mtext><mml:mtext> </mml:mtext><mml:mtext> </mml:mtext><mml:mtext> </mml:mtext><mml:mtext> </mml:mtext><mml:mtext> </mml:mtext><mml:mtext> </mml:mtext><mml:mtext> </mml:mtext><mml:mtext> </mml:mtext><mml:mtext> </mml:mtext><mml:mtext> </mml:mtext><mml:mtext> </mml:mtext><mml:mtext> </mml:mtext><mml:mtext> </mml:mtext><mml:mtext> </mml:mtext><mml:mtext> </mml:mtext><mml:mtext> </mml:mtext><mml:mtext> </mml:mtext><mml:mtext> </mml:mtext><mml:mtext> </mml:mtext><mml:mtext> </mml:mtext><mml:mtext> </mml:mtext><mml:mtext> </mml:mtext><mml:mfenced open="(" close=")"><mml:mrow><mml:mi>A</mml:mi><mml:mn>.2</mml:mn></mml:mrow></mml:mfenced></mml:mrow></mml:math>

Where the symbol Σ means fixing the mole fractions of all components except the nth while evaluating the differentiation

$$R_{i,i,j}^{L} = \frac{x_{ij}}{\rho_j^L a_j^I k_{i,m,j}^L} - \sum_{\substack{m=1 \\ m \neq i}}^{N} \frac{x_{i,j}}{\rho_j^L a_j^I k_{i,m,j}^L} \quad \text{for } i = 1,2,....n_c - 1, i \neq k \qquad (A.3)$$

<mml:math><mml:mrow><mml:msubsup><mml:mi>R</mml:mi><mml:mrow><mml:mi>i</mml:mi><mml:mo>,</mml:mo><mml:mi>k</mml:mi><mml:mo>,</mml:mo><mml:mi>j</mml:mi></mml:mrow><mml:mi>L</mml:mi></mml:msubsup><mml:mo>=</mml:mo><mml:mo>−</mml:mo><mml:msub><mml:mi>x</mml:mi><mml:mrow><mml:mi>i</mml:mi><mml:mo>,</mml:mo><mml:mi>j</mml:mi></mml:mrow></mml:msub><mml:mfenced open="(" close=")"><mml:mrow><mml:mfrac><mml:mn>1</mml:mn><mml:mrow><mml:msubsup><mml:mi>ρ</mml:mi><mml:mi>j</mml:mi><mml:mi>L</mml:mi></mml:msubsup><mml:msubsup><mml:mi>a</mml:mi><mml:mi>j</mml:mi><mml:mi>I</mml:mi></mml:msubsup><mml:msubsup><mml:mi>k</mml:mi><mml:mrow><mml:mi>i</mml:mi><mml:mo>,</mml:mo><mml:m

i>k</mml:mi><mml:mo>,</mml:mo><mml:mi>j</mml:mi></mml:mrow><mml:mi>L</mml:mi>
</mml:msubsup></mml:mrow></mml:mfrac><mml:mo>−</mml:mo><mml:mfrac><mml:
mn>1</mml:mn><mml:mrow><mml:msubsup><mml:mi>ρ</mml:mi><mml:mi>j</mml:mi>
<mml:mi>L</mml:mi></mml:msubsup><mml:msubsup><mml:mi>a</mml:mi><mml:mi>j</mml
:mi><mml:mi>I</mml:mi></mml:msubsup><mml:msubsup><mml:mi>k</mml:mi><mml:mrow>
<mml:mi>i</mml:mi><mml:mo>,</mml:mo><mml:mi>m</mml:mi><mml:mo>,</mml:mo><mm
l:mi>j</mml:mi></mml:mrow><mml:mi>L</mml:mi></mml:msubsup></mml:mrow></mml:mfra
c></mml:mrow></mml:mfenced><mml:mtext> </mml:mtext><mml:mtext> </mm
l:mtext><mml:mtext> </mml:mtext><mml:mtext> </mml:mtext><mml:mi>f</mm
l:mi><mml:mi>o</mml:mi><mml:mi>r</mml:mi><mml:mtext> </mml:mtext><mml:mte
xt> </mml:mtext><mml:mtext> </mml:mtext><mml:mi>i</mml:mi><mml:mo>=
</mml:mo><mml:mn>1</mml:mn><mml:mo>,</mml:mo><mml:mn>2</mml:mn><mml:mo>,</
mml:mo><mml:mn>....</mml:mn><mml:msub><mml:mi>n</mml:mi><mml:mi>c</mml:mi></m
ml:msub><mml:mo>−</mml:mo><mml:mn>1</mml:mn><mml:mo>,</mml:mo><mml:mt
ext> </mml:mtext><mml:mi>i</mml:mi><mml:mo>≠</mml:mo><mml:mi>k</
mml:mi><mml:mtext> </mml:mtext><mml:mtext> </mml:mtext><mml:mtext>&t
hinsp;</mml:mtext><mml:mtext> </mml:mtext><mml:mtext> </mml:mtext><mm
l:mtext> </mml:mtext><mml:mtext> </mml:mtext><mml:mtext> </mml:
mtext><mml:mtext> </mml:mtext><mml:mtext> </mml:mtext><mml:mtext>&thi
nsp;</mml:mtext><mml:mtext> </mml:mtext><mml:mtext> </mml:mtext><mml:
mtext> </mml:mtext><mml:mtext> </mml:mtext><mml:mtext> </mml:mt
ext><mml:mtext> </mml:mtext><mml:mtext> </mml:mtext><mml:mtext>&thinsp
;</mml:mtext><mml:mtext> </mml:mtext><mml:mtext> </mml:mtext><mml:mte
xt> </mml:mtext><mml:mtext> </mml:mtext><mml:mtext> </mml:mtext
><mml:mtext> </mml:mtext><mml:mtext> </mml:mtext><mml:mtext> </
mml:mtext><mml:mtext> </mml:mtext><mml:mtext> </mml:mtext><mml:mtext>
 </mml:mtext><mml:mtext> </mml:mtext><mml:mtext> </mml:mtext><
mml:mtext> </mml:mtext><mml:mtext> </mml:mtext><mml:mtext> </m
ml:mtext><mml:mtext> </mml:mtext><mml:mtext> </mml:mtext><mml:mtext>&
thinsp;</mml:mtext><mml:mtext> </mml:mtext><mml:mtext> </mml:mtext><m
ml:mtext> </mml:mtext><mml:mtext> </mml:mtext><mml:mtext> </mml
:mtext><mml:mtext> </mml:mtext><mml:mtext> </mml:mtext><mml:mtext>&thi
nsp;</mml:mtext><mml:mtext> </mml:mtext><mml:mtext> </mml:mtext><mml:
mtext> </mml:mtext><mml:mtext> </mml:mtext><mml:mtext> </mml:mt
ext><mml:mtext> </mml:mtext><mml:mtext> </mml:mtext><mml:mtext>&thinsp
;</mml:mtext><mml:mtext> </mml:mtext><mml:mtext> </mml:mtext><mml:mte
xt> </mml:mtext><mml:mtext> </mml:mtext><mml:mfenced   open="("
close=")"><mml:mrow><mml:mi>A</mml:mi><mml:mn>.4</mml:mn></mml:mrow></mml:mfe
nced></mml:mrow></mml:math>

- Mass flux for gas film

$$\left[\Gamma_{i,k,j}^{G} \right]\left(y_{j}^{I} - y_{j} \right) + \left[R_{j}^{G} \right]\left(N_{j}^{G} - N_{t}^{G} y_{j} \right) = 0 \qquad (A.5)$$

<mml:math><mml:mrow><mml:msubsup><mml:mi>Γ</mml:mi><mml:mrow><mml:mi
>i</mml:mi><mml:mo>,</mml:mo><mml:mi>k</mml:mi><mml:mo>,</mml:mo><mml:mi>j</m
ml:mi></mml:mrow><mml:mi>G</mml:mi></mml:msubsup><mml:mo>=</mml:mo><mml:msu
b><mml:mi>δ</mml:mi><mml:mrow><mml:mi>i</mml:mi><mml:mo>,</mml:mo><mml:
mi>k</mml:mi></mml:mrow></mml:msub><mml:mo>+</mml:mo><mml:msub><mml:mi>x</m
ml:mi><mml:mrow><mml:mi>i</mml:mi><mml:mo>,</mml:mo><mml:mi>j</mml:mi></mml:m
row></mml:msub><mml:msub><mml:mrow><mml:mfenced   open=""
close="|"><mml:mrow><mml:mfrac><mml:mrow><mml:mo>∂</mml:mo><mml:mi>ln
</mml:mi><mml:msubsup><mml:mi>ϕ</mml:mi><mml:mrow><mml:mi>i</mml:mi><mm
l:mi>j</mml:mi></mml:mrow><mml:mi>G</mml:mi></mml:msubsup></mml:mrow><mml:mro

w><mml:mo>∂</mml:mo><mml:msub><mml:mi>y</mml:mi><mml:mrow><mml:mi>i</mml:mi><mml:mo>,</mml:mo><mml:mi>j</mml:mi></mml:mrow></mml:msub></mml:mrow></mml:mfrac></mml:mrow></mml:mfenced></mml:mrow><mml:mrow><mml:msubsup><mml:mi>T</mml:mi><mml:mi>j</mml:mi><mml:mi>L</mml:mi></mml:msubsup><mml:mo>,</mml:mo><mml:msub><mml:mi>P</mml:mi><mml:mi>j</mml:mi></mml:msub><mml:mo>,</mml:mo><mml:mi>Σ</mml:mi></mml:mrow></mml:msub><mml:mtext> </mml:mtext><mml:mtext> </mml:mtext><mml:mtext> </mml:mtext><mml:mtext> </mml:mtext><mml:mtext> </mml:mtext><mml:mtext> </mml:mtext><mml:mtext> </mml:mtext><mml:mtext> </mml:mtext><mml:mtext> </mml:mtext><mml:mtext> </mml:mtext><mml:mtext> </mml:mtext><mml:mtext> </mml:mtext><mml:mtext> </mml:mtext><mml:mtext> </mml:mtext><mml:mtext> </mml:mtext><mml:mtext> </mml:mtext><mml:mtext> </mml:mtext><mml:mtext> </mml:mtext><mml:mtext> </mml:mtext><mml:mtext> </mml:mtext><mml:mtext> </mml:mtext><mml:mtext> </mml:mtext><mml:mtext> </mml:mtext><mml:mtext> </mml:mtext><mml:mtext> </mml:mtext><mml:mtext> </mml:mtext><mml:mtext> </mml:mtext><mml:mtext> </mml:mtext><mml:mtext> </mml:mtext><mml:mtext> </mml:mtext><mml:mtext> </mml:mtext><mml:mtext> </mml:mtext><mml:mtext> </mml:mtext><mml:mtext> </mml:mtext><mml:mtext> </mml:mtext><mml:mtext> </mml:mtext><mml:mtext> </mml:mtext><mml:mtext> </mml:mtext><mml:mtext> </mml:mtext><mml:mtext> </mml:mtext><mml:mtext> </mml:mtext><mml:mtext> </mml:mtext><mml:mtext> </mml:mtext><mml:mtext> </mml:mtext><mml:mtext> </mml:mtext><mml:mtext> </mml:mtext><mml:mtext> </mml:mtext><mml:mtext> </mml:mtext><mml:mtext> </mml:mtext><mml:mtext> </mml:mtext><mml:mtext> </mml:mtext><mml:mtext> </mml:mtext><mml:mtext> </mml:mtext><mml:mtext> </mml:mtext><mml:mtext> </mml:mtext><mml:mtext> </mml:mtext><mml:mtext> </mml:mtext><mml:mtext> </mml:mtext><mml:mtext> </mml:mtext><mml:mtext> </mml:mtext><mml:mtext> </mml:mtext><mml:mtext> </mml:mtext><mml:mtext> </mml:mtext><mml:mtext> </mml:mtext><mml:mtext> </mml:mtext><mml:mtext> </mml:mtext><mml:mtext> </mml:mtext><mml:mtext> </mml:mtext><mml:mtext> </mml:mtext><mml:mtext> </mml:mtext><mml:mtext> </mml:mtext><mml:mtext> </mml:mtext><mml:mtext> </mml:mtext><mml:mtext> </mml:mtext><mml:mtext> </mml:mtext><mml:mtext> </mml:mtext><mml:mtext> </mml:mtext><mml:mtext> </mml:mtext><mml:mtext> </mml:mtext><mml:mtext> </mml:mtext><mml:mtext> </mml:mtext><mml:mtext> </mml:mtext><mml:mtext> </mml:mtext><mml:mtext> </mml:mtext><mml:mtext> </mml:mtext><mml:mtext> </mml:mtext><mml:mtext> </mml:mtext><mml:mtext> </mml:mtext><mml:mtext> </mml:mtext><mml:mtext> </mml:mtext><mml:mtext> </mml:mtext><mml:mtext> </mml:mtext><mml:mtext> </mml:mtext><mml:mtext> </mml:mtext><mml:mtext> </mml:mtext><mml:mtext> </mml:mtext><mml:mtext> </mml:mtext><mml:mtext> </mml:mtext><mml:mtext> </mml:mtext><mml:mtext> </mml:mtext><mml:mtext> </mml:mtext><mml:mtext> </mml:mtext><mml:mtext> </mml:mtext><mml:mtext> </mml:mtext><mml:mtext> </mml:mtext><mml:mtext> </mml:mtext><mml:mtext> </mml:mtext><mml:mtext> </mml:mtext><mml:mtext> </mml:mtext><mml:mtext> </mml:mtext><mml:mtext> </mml:mtext><mml:mtext> </mml:mtext><mml:mtext> </mml:mtext><mml:mtext> </mml:mtext><mml:mtext> </mml:mtext><mml:mtext> </mml:mtext><mml:mtext> </mml:mtext><mml:mtext> </mml:mtext><mml:mtext> </mml:mtext><mml:mtext> </mml:mtext><mml:mtext> </mml:mtext><mml:mtext> </mml:mtext><mml:mtext> </mml:mtext><mml:mtext> </mml:mtext><mml:mtext> </mml:mtext><mml:mtext> </mml:mtext><mml:mtext> </mml:mtext><mml:mtext> </mml:mtext><mml:mtext> </mml:mtext><mml:mtext> </mml:mtext><mml:mtext> </mml:mtext><mml:mtext> </mml:mtext><mml:mtext> </mml:mtext><mml:mtext> </mml:mtext><mml:mtext> </mml:mtext><mml:mtext> </mml:mtext><mml:mtext> </mml:mtext><mml:mtext> </mml:mtext><mml:mtext> </mml:mtext><mml:mtext> </mml:mtext><mml:mtext> </mml:mtext><mml:mtext> </mml:mtext><mml:mtext> </mml:mtext><mml:mtext> </mml:mtext><mml:mtext> </mml:mtext><mml:mtext> </mml:mtext><mml:mtext> </mml:mtext><mml:mtext> </mml:mtext><mml:mtext> </mml:mtext><mml:mtext> </mml:mtext><mml:mtext> </mml:mtext><mml:mtext> </mml:mtext><mml:mtext> </mml:mtext><mml:mtext> </mml:mtext><mml:mtext> </mml:mtext><mml:mtext> </mml:mtext><mml:mtext> </mml:mtext><mml:mtext> </mml:mtext><mml:mtext> </mml:mtext><mml:mtext> </mml:mtext><mml:mtext> </mml:mtext><mml:mtext> </mml:mtext><mml:mtext> </mml:mtext><mml:mtext> </mml:mtext><mml:mtext> </mml:mtext><mml:mtext> </mml:mtext><mml:mtext> </mml:mtext><mml:mtext> </mml:mtext><mml:mtext> </mml:mtext><mml:mtext> </mml:mtext><mml:mtext> </mml:mtext><mml:mtext> </mml:mtext><mml:mtext> </mml:mtext><mml:mtext> </mml:mtext><mml:mtext> </mml:mtext><mml:mtext> </mml:mtext><mml:mtext> </mml:mtext><mml:mtext> </mml:mtext><mml:mtext> </mml:mtext><mml:mtext> </mml:mtext><mml:mtext> </mml:mtext><mml:mtext> </mml:mtext><mml:mtext> </mml:mtext><mml:mtext> </mml:mtext><mml:mtext> </mml:mtext><mml:mtext> </mml:mtext><mml:mtext> </mml:mtext><mml:mtext> </mml:mtext><mml:mtext> </mml:mtext><mml:mtext> </mml:mtext><mml:mtext> </mml:mtext><mml:mtext> </mml:mtext><mml:mtext> </mml:mtext><mml:mtext> </mml

:mtext><mml:mtext> </mml:mtext><mml:mtext> </mml:mtext><mml:mtext> </mml:mtext><mml:mfenced open="(" close=")"><mml:mrow><mml:mi>A</mml:mi><mml:mn>.6</mml:mn></mml:mrow></mml:mfenced></mml:mrow></mml:math>

Where the symbol Σ means fixing the mole fractions of all components except the nth while evaluating the differentiation

$$R^{G}_{i,i,j} = \frac{G_{ij}}{\rho^{G}_{j} a^{I}_{j} k^{G}_{i,m,j}} - \sum_{\substack{m=1 \\ m \neq i}}^{N} \frac{y_{i,j}}{\rho^{G}_{j} a^{I}_{j} k^{G}_{i,m,j}} \quad for \ i = 1, 2, ... n_{c} - 1, i \neq k \qquad (A.7)$$

$$R^{G}_{i,k,j} = -y_{i,j} \left(\frac{1}{\rho^{G}_{j} a^{I}_{j} k^{G}_{i,k,j}} - \frac{1}{\rho^{G}_{j} a^{I}_{j} k^{G}_{i,m,j}} \right) \quad for \ i = 1, 2, ... n_{c} - 1, i \neq k \qquad (A.8)$$

- Heat flux for the liquid film

$$a^{I}_{j} H_{j} \left(T^{I}_{j} - T^{L}_{j} \right) - q^{L}_{j} + \sum_{i=1}^{N} N^{L}_{i,j} \bar{H}_{i,j} = 0 \qquad (A.9)$$

- Heat flux for gas film

$$a^{I}_{j} h^{'}_{j} \left(T^{G}_{j} - T^{I}_{j} \right) - q^{G}_{j} + \sum_{i=1}^{N} N^{G}_{i,j} \bar{h}^{L}_{i,j} = 0 \qquad (A.10)$$

The rate-Based model uses well-known and accepted correlations to calculate binary mass transfer coefficients for the vapour and liquid phases, interfacial areas, heat transfer coefficients and liquid holdup. In general, these quantities depend on column diameter and operating parameters such as vapour and liquid flow rates, densities, viscosities, surface tension, and binary diffusion coefficients in both liquid and gaseous phases. Mass transfer coefficients, interfacial areas and liquid holdup also depend on the type, size, specific surface area, and construction material of packing and flow path length (packing tortuosity). Most parameters can vary by stage, but only depend on the properties for that stage. The subscript *j* on each variable is omitted in the equations for readability. The Onda model [18] predicts mass transfer coefficients and interfacial area for random packing.

<mml:math><mml:mrow><mml:msubsup><mml:mi>k</mml:mi><mml:mrow><mml:mi>i</mml:mi><mml:mo>,</mml:mo><mml:mi>k</mml:mi></mml:mrow><mml:mi>L</mml:mi></mml:msubsup><mml:mo>=</mml:mo><mml:mn>0.0051</mml:mn><mml:mtext> </mml:mtext><mml:mtext> </mml:mtext><mml:msup><mml:mrow><mml:mi>Re</mml:mi></mml:mrow><mml:mrow><mml:mn>0.667</mml:mn></mml:mrow></mml:msup><mml:mi>S</mml:mi><mml:msubsup><mml:mi>c</mml:mi><mml:mrow><mml:mi>L</mml:mi><mml:mo>,</mml:mo><mml:mi>i</mml:mi><mml:mo>,</mml:mo><mml:mi>k</mml:mi></mml:mrow><mml:mrow><mml:mo>−</mml:mo><mml:mn>0.5</mml:mn></mml:mrow></mml:msubsup><mml:msup><mml:mrow><mml:mfenced open="(" close=")"><mml:mrow><mml:msub><mml:mi>a</mml:mi><mml:mi>F</mml:mi></mml:msub><mml:msub><mml:mi>d</mml:mi><mml:mi>F</mml:mi></mml:msub></mml:mrow></mml:mfenced></mml:mrow><mml:mrow><mml:mn>0.4</mml:mn></mml:mrow></mml:msup><mml:msup><mml:mrow><mml:mfenced open="(" close=")"><mml:mrow><mml:mfrac><mml:mrow><mml:msup><mml:mi>μ</mml:mi><mml:mi>L</mml:mi></mml:msup><mml:mi>g</mml:mi></mml:mrow><mml:mrow><mml:msubsup><mml:mi>ρ</mml:mi><mml:mi>t</mml:mi><mml:mi>L</mml:mi></mml:msubsup></mml:mrow></mml:mfrac></mml:mrow></mml:mfenced></mml:mrow><mml:mrow><mml:mn>0.333</mml:mn></mml:mrow></mml:msup><mml:mtext> </mml:mtext><mml:mtext> </mml:mtext><mml:mtext> </mml:mtext><mml:mtext> </mml:mtext><mml:mtext> </mml:mtext><mml:mtext> </mml:mtext><mml:mtext> </mml:mtext><mml:mtext> </mml:mtext><mml:mtext> </mml:mtext><mml:mtext> </mml:mtext><mml:mtext> </mml:mtext><mml:mtext> </mml:mtext><mml:mtext> </mml:mtext><mml:mtext><

mml:mtext> </mml:mtext><mml:mtext> </mml:mtext><mml:mtext> </mml:mtext><mml:mtext> </mml:mtext><mml:mtext> </mml:mtext><mml:mtext> </mml:mtext><mml:mtext> </mml:mtext><mml:mtext> </mml:mtext><mml:mtext> </mml:mtext><mml:mtext> </mml:mtext><mml:mtext> </mml:mtext><mml:mtext> </mml:mtext><mml:mtext> </mml:mtext><mml:mtext> </mml:mtext><mml:mtext> </mml:mtext><mml:mtext> </mml:mtext><mml:mtext> </mml:mtext><mml:mtext> </mml:mtext><mml:mtext> </mml:mtext><mml:mtext> </mml:mtext><mml:mtext> </mml:mtext><mml:mtext> </mml:mtext><mml:mtext> </mml:mtext><mml:mtext> </mml:mtext><mml:mtext> </mml:mtext><mml:mtext> </mml:mtext><mml:mtext> </mml:mtext><mml:mtext> </mml:mtext><mml:mtext> </mml:mtext><mml:mtext> </mml:mtext><mml:mtext> </mml:mtext><mml:mtext> </mml:mtext><mml:mtext> </mml:mtext><mml:mtext> </mml:mtext><mml:mtext> </mml:mtext><mml:mtext> </mml:mtext><mml:mtext> </mml:mtext><mml:mtext> </mml:mtext><mml:mtext> </mml:mtext><mml:mtext> </mml:mtext><mml:mtext> </mml:mtext><mml:mtext> </mml:mtext><mml:mtext> </mml:mtext><mml:mtext> </mml:mtext><mml:mtext> </mml:mtext><mml:mtext> </mml:mtext><mml:mtext> </mml:mtext><mml:mtext> </mml:mtext><mml:mtext> </mml:mtext><mml:mtext> </mml:mtext><mml:mtext> </mml:mtext><mml:mtext> </mml:mtext><mml:mtext> </mml:mtext><mml:mtext> </mml:mtext><mml:mtext> </mml:mtext><mml:mtext> </mml:mtext><mml:mtext> </mml:mtext><mml:mtext> </mml:mtext><mml:mtext> </mml:mtext><mml:mtext> </mml:mtext><mml:mtext> </mml:mtext><mml:mtext> </mml:mtext><mml:mtext> </mml:mtext><mml:mtext> </mml:mtext><mml:mtext> </mml:mtext><mml:mtext> </mml:mtext><mml:mtext> </mml:mtext><mml:mtext> </mml:mtext><mml:mtext> </mml:mtext><mml:mtext> </mml:mtext><mml:mtext> </mml:mtext><mml:mtext> </mml:mtext><mml:mtext> </mml:mtext><mml:mtext> </mml:mtext><mml:mtext> </mml:mtext><mml:mtext> </mml:mtext><mml:mfenced open="(" close=")"><mml:mrow><mml:mi>A</mml:mi><mml:mn>.11</mml:mn></mml:mrow></mml:mfenced></mml:mrow></mml:math>

$$k_{i,k}^G = \begin{cases} 2.0 \, \text{Re}_G^{0.7} \, Sc_{G,i,k}^{0.333} a_F D_{i,k}^G \left(a_F d_F \right)^{-2} & for \ d_F < 0.015 \quad (A.12) \\ 5.23 \, \text{Re}_G^{0.7} \, Sc_{G,i,k}^{0.333} a_F D_{i,k}^G \left(a_F d_F \right)^{-2} & for \ d_F > 0.015 \quad (A.13) \end{cases}$$

$$a^I = a_w A h_F \qquad (6-27)$$

$$a_w = a_F \left[1 - \exp\left(-1.45 \left(\frac{\sigma_c}{\sigma} \right)^{0.75} \text{Re}_L^{0.1} \, Fr_L^{-0.05} We_L^{0.2} \right) \right] \qquad (A.14)$$

The heat transfer coefficient h was estimated by Chilton–Colburn method [42]

$$h_j = \overline{k}_j \overline{\rho}_j C_{p_j} \left(\frac{\lambda_j}{\overline{D}_j \overline{\rho}_j C_{p_j}} \right)^{2/3} \tag{A.15}$$

$$where \ \overline{D}_j = \frac{\sum_{i=1}^{nc-1} \sum_{k=i+1}^{nc} (x_{i,j} + \delta)(x_{k,j} + \delta) D_{i,k,j}}{\sum_{i=1}^{nc-1} \sum_{k=i+1}^{nc} (x_{i,j} + \delta)(x_{k,j} + \delta) D_{i,k,j}} \tag{A.16}$$

$$and \ \overline{k}_j = \frac{\sum_{i=1}^{nc-1} \sum_{k=i+1}^{nc} (x_{i,j} + \delta)(x_{k,j} + \delta) k_{i,k,j}}{\sum_{i=1}^{nc-1} \sum_{k=i+1}^{nc} (x_{i,j} + \delta)(x_{k,j} + \delta) D_{i,k,j}} \tag{A.17}$$

Where C_p is the specific molar heat capacity, $\overline{D}$ is the average diffusivity, $\overline{k}$ is the average mass transfer coefficient, $\overline{\rho}$ is the averaged density, M is the molecular weight, u is the average flow velocity, ρ is the molar density, λ is the thermal conductivity, n_c is the number of components and d is the Chilton-Colburn averaging parameter specified on the Rate-Based Setup Specifications sheet with a default recommended value of 0.0001. This parameter provides stability when compositions change, especially in reactive systems when some compositions may go to zero at the boundary.

The pressure drops through the Dixon packing were estimated using literature models applied to random Raschig packing as follows [41].

$$\Delta P / L = C_{P,0} \left(\frac{64}{Re_V} + \frac{1.8}{Re_V^{0.08}} \right) \frac{a}{\varepsilon^3} \frac{u_V^2 \rho}{2} \left(1 + \frac{2}{3} \frac{1}{1-\varepsilon} \frac{d_p}{d_s} \right) \tag{A.18}$$

$$\frac{1}{Re_V} = \frac{(1-\varepsilon) v_V}{u_V d_p} \left(1 + \frac{2}{3} \frac{1}{1-\varepsilon} 6 \frac{1-\varepsilon}{a} \frac{1}{d_s} \right) \tag{A.19}$$

$$d_p = 6 \frac{1-\varepsilon}{a} \tag{A.20}$$

<REF>References
<BIBL>
[1] D. Greneche, W.J. Szymczak,;1; The AREVA HTR Fuel Cycle: An analysis of technical issues and potential industrial solutions, Nucl. Eng. and Des. 336 (2006) 635-642.

[2] A. Bruggeman, J. Braet, S. Vanderbiesen;1; and JET EFDA Contributors. Water Detritiation: better catalysts for liquid phase catalytic exchange, 7th Tritium Science and Technology Conference, <PL>Baden Baden, Germany</PL> 12-17 September 2004

[3] S. R. Sherman, T. M. Adams,;1; Tritium Barrier Materials and Separation Systems for the NGNP, Prepared for the NGNP Project under MPO 00072051, Battelle Energy Alliance, <PL>Savannah</PL> River National Laboratory, August 2008

[4] T. Sugiyama, Y. Asakura, Y. Udaa, T. Shiozaki, Y. Enokida, I. Yamamoto,;1; Present status of hydrogen isotope separation by CECE process at the NIFS, Fusion Eng. Des. 81 (2006) 833-838

[5] A. N. Perevezentsev, A. C. Bell,;1; Wet scrubber column for air detritiation, Fusion Sci. Technol. 56 (2009) 1455-1461

[6] A. N. Perevezentsev, A. C. Bell,;1; Development of water detritiation facility for JET, Fusion Sci. Technol. 53 (2008) 816-829

[7] F. Huang, C. Meng,;1;Method for the Production of Deuterium-Depleted Potable Water, Ind. Eng. Chem. Res. 50 (2001) 378-381

[8] M. Benedict, T. H., H. W. Levi,;1; Nuclear Chemical Engineering; <PL>McGraw-Hill </PL> <PN>Book Company</PN>, 1980

[9] W. H. Stevens,;1; Process and catalyst for enriching a fluid with hydrogen isotopes, Canadian Patent (1972) No.907292

[10] M. N. tSaoir, J. Sa, D. L. A. Fernandez, M. McMaster, C. Hardacre, K. Kitagawa, F. Aiouache,;1; Visualization of water vapour flow in a packed bed adsorber by near-infrared diffused transmittance tomography, Chem. Eng. Sci. 66 (2011) 6407-6419

[11] M. N. tSaoir, D. L. A. Fernandez, M. McMaster, C. Hardacre, K. Kitagawa, F. Aiouache,;1; Transient distributions of composition and temperature in a gas–solid packed bed reactor by near-infrared tomography, Chem. Eng. J. 189-190 (2012), 383– 392

[12] I. Cristescu, I. R. Cristescu, L. Dörr, M. Glugla, G. Hellriegel, R. Michling, D. Murdoch, P. Shaffer, S. Welte, W. Wurster,;1; Commissioning of water detritiation and cryogenic distillation systems at TLK in view of ITER, Fusion Eng. Des. 82 (2007) 2126-2132

[13] S. Paek, D. H. Ahn, H. J. Choi, K. R. Kim, M. Lee, S. P. Yim,;1; The performance of a trickle-bed reactor packed with a Pt/SDBC catalyst mixture for the CECE process. Fusion Eng. Des. 82 (2007) 2252-2258

[14] A. S. Sumchenko, A. N. Bukin, S. A. Marunich, Y. S. Pak, M. B. Rozenkevich, I. L. Selivanenko,;1; Influence of Packing Columns Starting Modes on Effectiveness of Processes of Water Rectification and Detritiation of Gases by the Method of Phase Isotopic Exchange. Theoretical Foundations of Chemical Engineering 49 (2015) 252-260

[15] A. Perevezentsev, A. C. Bell, P. D. Brennan, J. L. Hemmerich,;1; Measurement of Pressure Drop and HETP in Columns Packed with Different Hydrophobic Catalysts for Tritium Isotopic Exchange Between Water and Hydrogen, Fusion Sci. Technol. 41 (2002) 1102-1106

[16] I. Cristescu, U. Tammb, M. Glugla, Caldwell-Nichols,;1; C J. Investigation of simultaneous tritium and deuterium transfer in a catalytic isotope exchange column for water detritiation, Fusion Eng. Des.61 (2002) 537-542

[17] R. Kumar, S. Mohan, S. M. Mahajani,;1; Reactive Stripping for the Catalytic Exchange of Hydrogen Isotopes. Ind. Eng. Chem. Res. 52 (2013) 10935-10950

[18] K. Onda, H. Takeuchi, Y. Okumoto,;1; Mass transfer coefficients between gas and liquid phases in packed columns. J. Chem. Eng. Jpn. 1 (1968) 56-62

[19] O. Fedorchenko, I. Alekseev, V. Uborsky,;1; Water-Hydrogen Isotope Exchange Process Analysis, Fusion Sci. Technol. 54 (2008) 450-453

[20] T. Yamanishi, K. Okuno,;1; Simulation code treating all twelve isotopic species of hydrogen gas and water for multistage chemical exchange column, <PL>Japan</PL> Atomic Energy Research Institute 1994, JAERI-Data Code, 94-019

[21] L. Ye, LD. Luo, T. Tang, W. Yang, P. Zhao,;1; Process simulation for hydrogen/deuterium exchange in a packed column, International Journal of Hydrogen Energy 39 (2014) 6604-6609

[22] R. Taylor, R. Krishna,;1; Multicomponent mass transfer; <PN>Wiley</PN>: <PL>New York</PL>, 1993

[23] M. Kinoshita,;1; An Efficient Simulation Procedure Especially Developed for Hydrogen Isotope Distillation Columns, Fusion Sci. Technol. 6 (1984) 574-583

[24] M. N. tSaoir, M.N.; Fernandes, D.L.A.; Sa, J.; Kitagawa, K.; Hardacre, C.; Aiouache, F.,;1; Three dimensional water vapour visualization in porous packing by near-infrared diffuse transmittance tomography, Ind. Eng. Chem. Res. 2012, 51, 8875-8882

[25] F. Alzahrani, M. Aldehani, H. Rusi, M. McMaster, D. L. A. Fernandes, S. Assabumrungrat, M. N. tSaoir, F. Aiouache,;1; Gas Flow visualization in low aspect ratio packed beds by three-dimensional modeling and near-infrared tomography, Ind. Eng. Chem. Res. 51 (2015) pp 12714–12729

[26] T. F. Roland, J. Borysow, M. Fink,;1; Surface mediated isotope exchange reactions between water and gaseous deuterium, Journal of Nuclear Materials 353 (2006) 193-201

[27] K. Kawakami, Y. Takao, K. Kusunoki,;1; Kinetics of Isotopic Exchange Reaction between Hydrogen and Water Vapor over Platinum Supported on a Hydrophobic Carrier, *Can. J. Chem. Eng.* 64 (1986) 432-439

[28] N. H. Sagert, M. L. Pouteau,;1; The Production of Heavy Water: Hydrogen-Water Deuterium Exchange over Platinum Metals on Carbon Supports, Platinum Met. Rev. 19 (1975) 16-21

[29] A. Richardson, J. W. Leachman,;1; Thermodynamic properties status of deuterium and tritium, Advances in Cryogenic Engineering, AIPConf. Proc. 2012 1434, 1841-1848

[30] P. C. Souers,;1;Hydrogen Properties for Fusion Energy, University of California Press, Berkley, 1986

[31] W. A. Van Hook, L. P. N. Rebelo, M. Wolfsberg,;1; Isotope effects on VLE properties of fluids and corresponding states:Critical point shifts on isotopic substitution, Fluid Phase Equilibria 257 (2007) 35-52

[32] G. Vasaru,;1; Tritium Isotope Separation; CRC Press, 1993

[33] J. Cho, S.Cho, S. Yun, M. H. Chang, H. Kang, K. J. Jung, D. M. Kim,;1; Estimation of Physical Properties for Hydrogen Isotopes Using Aspen Plus Simulator, Transactions of the Korean Nuclear Society Spring Meeting, <PL>Jeju, Korea,M</PL>ay 22, 2009, 135-136

[34] S. Noh, J. Rho, J. Cho,;1; Cryogenic Distillation Simulation for Hydrogen Isotopes Separation, Journal of the Korea Academia-Industrial cooperation Society 14 (2013) 4643-4651

[35] M. Sdomon,;1; Thermodynamic properties of liquid H_2O and D_2O and their mixtures, Electronics Research Centre Cambridge, Mass., National Aeronautics and Space Administration, NASA TN D-5223, <PL>Washington, D. C</PL>. 1969

[36] A. Durmayaz,;1; Approximate functions for the fast computation of the thermodynamic properties of heavy water, Nuclear Engineering and Design 178 (1997) 309-329

[37] H. W. Xianga,;1; Vapor Pressure and Critical Point of Tritium Oxide, J. Phys. Chem. Ref. Data 32 (2003) 1707-1711

[38] N. Matsunaga, A. Nagashima,;1; Saturation Vapor Pressure and Critical Constants of H_2O, D_2O, T_2O, and Their Isotopic Mixtures, International Journal of Thermophysics 8 (1987) 681-694.

[39] A. S. Friedman, D. White, H. L. Hohnston,;1; Critical Constants, Boiling Points, Triple Point Constants, and Vapor Pressures of the Six Isotopic Hydrogen Molecules, Based on a Simple Mass Relationship, J. Chem. Phys. 19 (1951) 126-127

[40] J. H. Rolston, J. D. Hartog, J. P. Butler,;1; The Deuterium Isotope Separation Factor between Hydrogen and Liquid Water, J. Phys. Chem. 80 (1976)1064−1067.

[41] R. Billet, M. Schultes,;1; Prediction of Mass Transfer Columns with Dumped and Arranged Packings: Updated Summary of the Calculation Method of Billet and Schultes, Chem. Eng. Res. Des. 77 (1999) 498-504

[42] T. Chilton, A. P. Colburn,;1; Mass Transfer (Absorption) Coefficients Prediction from Data on Heat Transfer and Fluid Friction, Ind. Eng. Chem. 26 (**1934**) 1183-1187

[43] T. Sugiyama, A. Ushida, I. Yamamoto,;1; Effects of the gas-liquid ratio on the optimum catalyst quantity for the CECE process with a homogeneously packed LPCE column, Fusion Eng. Des. 83 (2008) 1447-1450

[44] O. A. Fedorchenko, I. A. Alekseev, A. S. Tchijov, V. V. Uborsky,;1; Modeling of the Process of Three-Isotope (H, D, T) Exchange Between Hydrogen Gas and Water Vapour on Pt-SDBC Catalyst over a Wide Range of Deuterium Concentration, Fusion Sci.Technol. 48 (2005) 120-123

</BIBL>

<Figure>Fig. 1 Schematic representations of the three mass transfer models: (a) Chemical equilibrium and gas/liquid physical equilibrium (CEPE) model, (b) Chemical kinetics and gas/liquid physical equilibrium (CKPE) model, (c) Chemical kinetics and rate-based gas/liquid non-equilibrium (CKRN-E) model

<Figure>Fig. 2. Scheme of the whole tomography apparatus, packed bed tube diameter: 12 mm, thickness of both tubes: 1 mm, Evaporator (Bronkhorst) = Mass flow controller (N_2), air-actuated switching valve, distilled water bath; H: Humidity sensor; TC_1= Thermocouples (monitoring), TC_2: Thermocouples connected to programmable temperature controllers; MS: Mass spectrometer

<Figure>Fig. 3 Kinetic model for deuterium isotopic exchange. (a) Transient composition profiles of deuterium isotopologues in both hydrogen gas and water vapour, feed flow rate: 0.338 L/min, compositions of D_2O, H_2 and N_2: 12, 25 and 63 %, respectively, temperature: 323 K, (b) chemical equilibrium constants with temperature, (c) Steady-state composition profiles of products of deuterium isotopologues with residence time in both hydrogen gas and water vapour, compositions of D_2O, H_2 and N_2: 12, 25 and 63 %, respectively, temperature: 323 K, (d) Steady-state composition profiles of products of deuterium isotopologues with temperature in both hydrogen gas and water vapour, Feed flow rate: 0.338 L/min, compositions of D_2O, H_2 and N_2: 12, 25 and 63 %, respectively, temperature: 323 K, (e) Arrhenius plots of chemical rate constants

<Figure>Fig. 4 Product distribution at the top (a-d) of the LPCE column and inside the LPCE column (e) by phase equilibrium modelling. Liquid feed composition: 0.2 mol % of D_2O, Pure hydrogen gas, liquid flow are L': 3.5 mol/h, column ID: 0.025 m, height: 1.2 m, packing type: Dixon ring of 1.5 mm. (a) Effect of pressure and temperature, (b) Effect of gas to liquid flowrate ratio, (c) Effect of reactive stages, (d) Effect of mass of catalyst per stage, T=333 K, G'/L'=1, P= 101.3 kPa and (e) product distribution inside the LPCE column, T=333 K, G'/L'=1, P= 101.3 kPa

<Figure>Fig. 5 Product distribution by rate-based non-equilibrium phase model: (a_1, a_2 and b) at the top of the LPCE column. (b_1) profiles of kinetic rate constants $k_{r,4}$, liquid/gas overall mass transfer coefficient based on the gaseous phase for D_2O species $K_{G, D2O}$, and gas/liquid exchange rate constant $K_{g, overall}$. (b_2) Ratio of kinetic rates of D_2O to mass transfer rate of D_2O. (c_1 and c_2) effect of gas to liquid flow rate at L': 3.5 mol/h and liquid to gas flow rate at G'= 3.5 mol/h, respectively. (d) Product distribution and relevant reaction rates inside the LPCE column.
Operating conditions: (a_1) and (b-d): Liquid feed composition: 0.2 mol % of D_2O, Pure hydrogen gas, liquid flow are L': 3.5 mol/h, column ID: 0.025 m, height: 1.2 m, packing type: Dixon ring of 1.5 mm. (a_2) Column diameter = 40 mm, diluted Raschig ring reactive packing into an inert packing at 50%, G'= 1.2 L (STP)/h, T = 323 K

<Figure>Fig. 6 (a) Product distributions inside the LPCE column by the size of Dixon packing, (b) Product distributions inside the LPCE column by type of packing arrangement (layered or mixed packing) and (c) Product distributions inside the LPCE column in presence of tritium and (d) effect of deuterium content on mass transfer coefficients based on the gaseous phase K_G.
Operating conditions: (a, b) Liquid feed composition: 0.2 mol % of D_2O, Pure hydrogen gas, liquid flow are L': 3.5 mol/h, column ID: 0.025 m, height: 1.2 m, packing type: Dixon ring of 1.5 mm and 6 mm particle. (c, d) Liquid feed compositions: 30.3 Bq/cm^3 of HTO and 2.5 mol % of HDO, Hydrogen gas compositions: 0.4 mol % of HD, liquid flowrate: 120 cm^3/h, Hydrogen flow rate: 0.5 m^3/h, T= 338 K.
TDENDOFDOCTD